Department of Precision and Microsystems Engineering

Designs for rotary shaft fluid seals in an aqueous environment using ferrofluid

O.G.R. Potma

Report no : 2017.057
Coach : ir. S.G.E. Lampaert
Professor : Prof. dr. ir. J.L. Herder
Specialisation : Mechatronic System Design
Type of report : Master Thesis
Date : November 23, 2017

Designs for rotary shaft fluid seals in an aqueous environment using ferrofluid

by

O.G.R. Potma

to obtain the degree of **Master of Science**
at the Delft University of Technology,
to be defended publicly on Thursday November 23, 2017 at 13:30.

Student number:	4007824	
Project duration:	September 2016 – November 2017	
Thesis committee:	Prof. dr. ir. J. L. Herder,	TU Delft, Chairman
	ir. S. G. E. Lampaert,	TU Delft, Supervisor
	dr. R. Delfos,	TU Delft
	ing. R. van Herwaarden,	Ægir Marine

An electronic version of this thesis is available at `http://repository.tudelft.nl/`.

TU Delft Delft University of Technology

"Precision instruments are designed to achieve an idea, dimensional precision, whose perfection is impossible. There is no perfectly shaped part of the motorcycle and never will be, but when you come as close as these instruments take you, remarkable things happen, and you go flying across the countryside under a power that would be called magic if it were not so completely rational in every way."

Robert M. Pirsig, Zen and the Art of Motorcycle Maintenance

Preface

The engineering concept of sealing is a fascinating subject and in no way could I have predicted that I would end my studies on such a subject. To go from such a broad start at the mechanical engineering bachelor to end up in such a small niche of science and engineering has been quite a trip. Sealing rotary shaft using ferrofluid sees the clash of two virtually opposite worlds; The maritime industry, a monolith of old age and reliable technology, and the high-tech world with its (quite literally) space age and ever -changing technology of ferrofluids. Seeing a company brave enough to dip its toes in unfamiliar waters for the dream of out-competing all others is inspirational.

This technology has the potential to not only be an improvement on wear reduction on parts that force a ship into the dry dock for maintenance, but could also to have a positive impact on the environmental stress that current sealing technology produces. I am glad to have participated in this subject and would love to see the fruition of this technology in the nearby future.

Acknowledgements

Hereby I would like to express my gratitude to everyone who has contributed, directly or indirectly, to the realisation of this thesis

I would like to thank my girlfriend Elena Piët for her insights, our discussions and her dedications on matters going far beyond just this subject alone. Keeping me critical of life, love and knowledge has brought me to where I am.

I would like to thank my coach Stefan Lampaert for providing me with a subject that has incurred a lot of joy, fascination, frustration, mistakes and victories. I really appreciate the amount of time and effort you put into discussing with me the many hurdles the thesis brought and for being critical of the work I did.

I would like to thank Ron van Ostayen for his supervision of our undergraduate group of thin film technology. Your years of experience gave an extra dimension to our already complex specialisation. For me it was a delight to listen and contribute to each others subjects presented during these meetings by students and PhD's.

I would like to thank the people from our office we worked in at the TU, namely Bram, Bas, Boran, Jan, Simon, Sarah, Nils and Sander. I enjoyed the stories, lunches, walks and drinks we had together. Building graduation gifts for each other has been a lot of fun and I couldn't think of a better environment to finish my thesis.

I would like to thank al of the technical staff of PME and 3mE that have helped me in creating the setups used for this thesis. To the people Rob, Harry, Patrick, Spiridon, Gerard, Rene and Wim I say thank you for all your time and experience.

I would like to thank my family for their love and patients during my studies. The opportunities I was able to take thanks to you have given me the qualities with which I was able to attend the university that suited my curiosities so nicely.

I would like to thank the whole of PME, from all the employees working hard to keep the quality of the master as high as possible, to the students that chose to attend the master. It has been one of the most inspirational places I have ever been a part of in a field that I did not know beforehand I would enjoy so much.

I would like to thank the proofreaders of my thesis for giving the thesis the linguistic improvements that it needed. To Patricia Heintz, Claire Parment and Wiebe van Geest I say thank you for the time you took in reading and correcting my mistakes.

Finally, I would like to thank Ægir Marine for their insights from a industrial perspective. It was very enlightening to see the direct interest of a company in academic research and trying to convey that knowledge into a practical solution.

Abstract

Seals are used throughout the technology spectrum to prevent products from leaving their container or preventing foreign products from entering. With the sealing of rotary parts like shafts, the seal needs to not only provide sealing capabilities, but also simultaneously allow for the desired movement without too much friction or wear. This is often accomplished using rubber rings in combination with lubricating oils. This technology, even though its design is effective, has not changed for over 80 years. The introduction of ferrofluid has tried to change that since the 70s.

Ferrofluid is attracted to magnets by its magnetic properties. It consists of very small coated magnetite particles suspended colloidally in a carrier. Because it remains a fluid when magnetic fiels are close-by, and because these fields increase the internal pressure of the fluid, ferrofluid can be used as a seal on a shaft by creating an uninterrupted liquid ring around said shaft.

This thesis focuses on the design and physics of ferrofluid seals. The pressure difference the seal can handle is determined by the magnetic field intensity where the seal is present and the saturation level of the ferrofluid. These parameters are improved by magnet type, field guidance, polepieces and ferrofluid type. The size of the gap between the shaft and the polepiece and the geometry of the piece are also of importance regarding sealing capacity. Lastly, hydrodynamics play an important role in the stability of the seal. The speed of the fluid can lead to jettisoning, due to centripetal forces or to mixing with the medium it is in contact with, which limit sealing capacity. Correct seal design can prevent this.

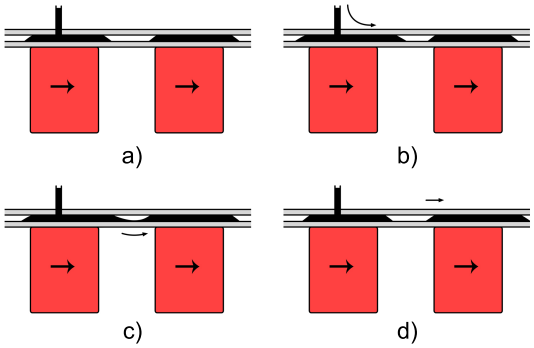

Figure 1: Transport of FF. The seal is first a) at equilibruim. Then FF is added b) to the first seal, moving the interface. Magnetic forces c) of the second magnet become stronger, pulling excess fluid towards it. Finally equilibrium restores d) with the excess fluid now on the second magnet

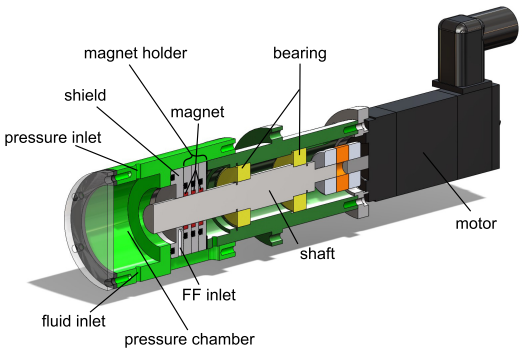

Figure 2: A cutthrough of the *FFP 02*. Colours and tags are used to differentiate between the different components.

A major problem with ferrofluid seals is that when the medium to seal is (sea)water, the fluid tends to degrade over time and this leads the seal to fail. The liquid reacts with the particles or carrier, causing a deterioration of the ferrofluids properties. Research shows a seal life time of

roughly 300 days can be obtained, as opposed to rubber lip seals which hold out for several years.

A method described in this thesis is used to extend the seal's lifetime. This method consists in pumping *fresh* ferrofluid into the front end of the seal, letting it mix and pushing the *older, partially degraded* ferrofluid out towards the back end of the seal, thus preventing the seal from failing due to degradation. To prove the method, two experiments have been devised. The first experiment discusses the transport of ferrofluid over several seals in sequence in a static 2-dimensional setup (figure 1) and the pressure drop capacity of the setup. The second experiment is an extention of the previous experiment in a setup with a rotating shaft and discusses the influence of shaft speed and water on the seal life while having ferrofluid transport (figure 2).

The analytical method of determining the critical pressure was experimentally confirmed to a high degree of conformity. The critical pressure for the dynamic case followed a descending trend that was predicted to happen (figure 6.6). At sub critical pressures, the results show that in the static case, with a FF/air interface, ferrofluid can be added to the seal configuration and successfully transported over the successive sealing elements. In the dynamic case the same results where observed, showing no drop in pressure at different speed increments. The results demonstrate that the seal functions as based on the design criteria from literature.

With a FF/water interface the setup demonstrated a lifetime of 51 minutes. When performing the FF transport test, a leak was detected when the ferrofluid was added to the seal at higher speeds (3000 RPM). The time until failure was significantly shorter compared to the lifetime. The flow rate of the FF addition was suggested to be the main culprit.

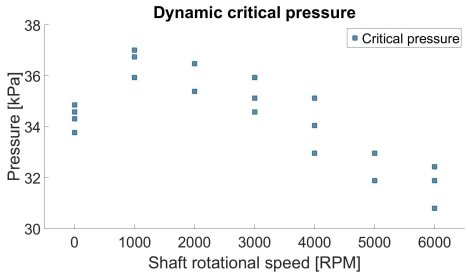

Figure 3: At each speed interval a leak test was carried out, resulting in the $p_{c,d}$. The slope indicates the $p_{c,d}$ decreases with speed increase.

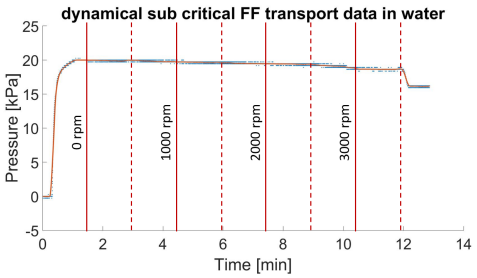

Figure 4: Set up is filled with water and pressurized to $0.5p_{c,s}$. At certain moments (solid line) speed is increased, and inbetween (dotted line) FF is added to the seal. At 3000 RPM the seal fails at the moment of FF addition.

The thesis has demonstrated that ferrofluid transport can be a viable method of maintaining and prolonging the lifetime of ferrofluid seals in an aqueous environment, making the possibility of liquid seals for commercial use in ships and machinery more of a reality.

Contents

List of Figures

List of Tables

Chapter 1

Project introduction

1.1 Research background

1.1.1 Ferrofluids

Ferrofluid has been around since the 1960s, initially researched at the NASA Research Center to aid in the transport of rocket fuel and other fluids in zero gravity. Consisting of very small coated magnetite particle in a carrier fluid, ferrofluid is attracted by magnetic fields, altering certain properties (internal pressure, viscosity) but remaining fluid. These fields become somewhat visible when saturating the magnetization of the fluid, as can be seen in figure 1.1. Existing of only these few ingredients, ferrofluid is relatively inexpensive to produce.

These fascinating fluids, soon after their discovery, harboured a multitude of possible applications, like in the use of linear contactless bearings, from commercially available speaker to high precision equipment [17]. Having no mechanical contact (that is, no solid parts moving over each other) reduces issues like vibration transmission, stick-slip, friction and eliminates wear. These features have also led to other applications, already researched as far back as the 1970s. The internal build-up of pressure in the fluid means that, if applied correctly, it can withstand an external pressure from a gas by using the fluid itself as a barrier. Ferrofluid therefore can also be used in the design of a seal.

1.1.2 Seals

The basics of a seal is preventing fluids from entering or escaping certain enclosures and to be able to hold this to a certain pressure (think of the cap on a beer bottle). But when sealing moving objects like the shaft of a machine in a demanding environment like a washing machine or ship, the challenge is increased. Conventionally a mechanical ring made of rubber (figure 1.2), sometimes in combination with pressurized oil, is used to exclude fluids by fitting snugly around the shaft, but leaving the shaft free to move. This unfortunately causes massive wear on the shaft over time or leakage of the oil into the environment.

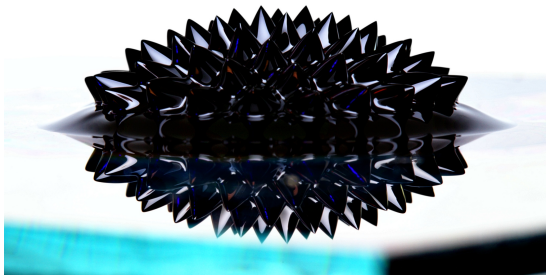

Figure 1.1: Picture of ferrofluid in proximity of a magnet. The spikes indicate saturation of the magnetization. Taken from https://commons.wikimedia.org/wiki/File:Ferrofluid_large_spikes.jpg

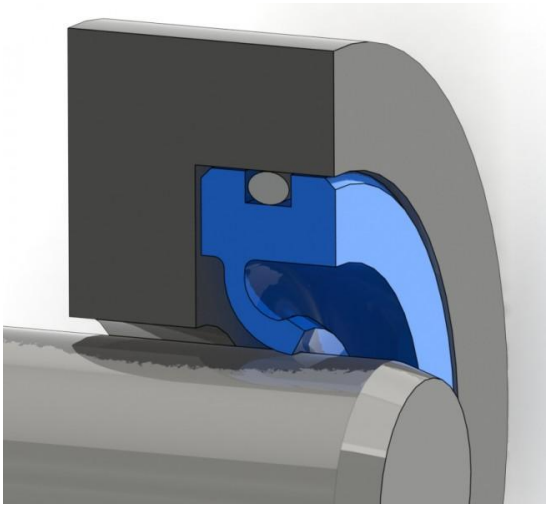

Figure 1.2: A 3D modeled cutthrough of a basic lip seal. Taken from http://www.ceetak.com/case-studies/university-of-sheffield-case-study/

A ferrofluid seal would distinguish itself by being contactless, needing no pump to maintain a fluid pressure and having virtually no leakage (magnetic fluid stays with the magnet). For ships, a technology like this could greatly reduce the amount of time needed in dry dock for repair and replacement of shaft components since the seal would not be worn out.

1.2 Problem definition

The technology over time has yielded many innovations and patents, specifically in sealing gasses and vacuums, but has at present not been able to create reliable long life seals for excluding liquids. Literature on the subject has shown that for a seal in contact with water the seal fails within a short amount of time. A lot can be solved by correct seal design, but the problem of failure by ferrofluid degradation still remains. Solutions exist to extend the lifetime of the fluid, but these fall short of being able to compete with conventional methods. The goal of this thesis is to explore the prospect of designing a seal that has a significant longer lifetime and possibly degradation based failures.

- How does degradation of FF lead to seal failure in the dynamic case with a water interface
- Is it possible to extend seal lifetime or to prevent its failure.

1.3 Thesis objective

Now that the problem is defined, the objective of this thesis can be formulated. The objective will be to design a seal using a ferrofluid that has a mechanism to prevent the degrading ferrofluid from negatively influencing the lifetime of the seal. The objective is devised as such:

- To identify the design parameters for the ferrofluid seal.
- To devise a method to replace the degraded ferrofluid in the seal.
- To build a demonstrator to test said method.

1.4 Thesis structure

The structure of the thesis can be divided into three parts; First, an introduction where the general background on ferrofluid and ferrofluid seals research is discussed. This will be covered in chapters 2, 3 and 4. Chapter 2 contains information on the fundamentals of ferrofluid seals, detailing the basic workings of the fluid as well as mechanical and hydrodynamical properties directly attributed to seals. Chapter 3 addresses the general principles involved in designing ferrofluid seals. It mentions the basic parts of a seal, its major parameters and the functionality of the magnet. Chapter 4 deals with a selection of important scientific work on the subject of ferrofluid seals and also with patents.

The second part addresses how to solve the problem definition as stated above using the information obtained in the first part . This is written in the form of two scientific papers and is covered in chapters 5 and 6. Chapter 5 discusses the design of a static seal configuration for passive ferrofluid transport. Chapter 6 discusses a dynamic design of a similar seal configuration for passive ferrofluid transport.

The third part will be a discussion on the results obtained in the second part and compared to the problem definition, as well as a conclusion of the previous parts and future recommendations. Lastly the part will contain appendices with more in-depth information on certain subjects within the thesis. This can be found in chapters 7, 8 and the appendices.

Chapter 2

Fundamental properties of ferrofluid seals

This chapter will provide a deeper understanding of the physics of magnetic fluids in general and their behaviour in an engineering sense. The first section will briefly explain magnetic fluids, followed by a section on fluid interface instability and pressure build-up of FF by the introduction of a magnetic field. Lastly there will be a section on basics of magnetic behaviour of FF's.

2.1 Basics on Magnetic fluids

Magnetic fluids come in all shapes and sizes, depending on the application. The fluid is a suspension of small magnetizable particles in a carrier. The carrier can virtually be any liquid, here again depending on the application. Within this scope the fluid should not be non-miscible in water and the fluid should be colloidal stable.

The term colloid is used to categorise a suspension mixture where the particles are in the order of $1 - 1000\mu m$ and do not sediment or aggregate at equilibrium, i.e. colloidal stable. The interactions that make a suspension colloidal are the thermal energy E_{therm}, gravitational energy E_{grav} and dipole energy E_{dip} of the particles [17]. The thermal energy forces the particles apart whilst the other energies pull them in one direction or towards each other respectively. For stability to exist, these energies have to be of the same order of magnitude.

With magnetic fluids the magnetic energy E_{mag} also interacts with the suspension. This occurs when the particles have paramagnetic properties. According to Tipler [18], this means the particle material has permanent magnetic moments that only very weakly interact with each other , resulting in a very small, positive magnetic susceptibility χ_m. The particles further tend to stick to each other (aggregation). Aggregation of particles also occurs due to the van der Waals interaction. This can be prevented by providing the particles with an electric charge stabilization or by coating the particles with long chained organic molecules [19]. These methods repulse and prevent particles from coming into contact with one another.

The particles, being paramagnetic, are randomly oriented in the carrier. When an external magnetic field is applied to the colloid, the rheological properties change. Chain formation occurs, which is another form of aggregation, and the particles are reoriented to be aligned with the field. Chains are particles lining up in parallel to the field and linking to one another. The degree in which the particles align and the length of the chains are also prescribed by the previously mentioned energy differences, combined with the use of a coating. The degree of reorientation is determined by the interactions between the magnetic alignment torque and the shear related rotational torque. The chain formation, alignment and reorientation are categorised in literature as the *magnetoviscous effect* [20] and have been modelled in [17].

The magnetization of a magnetic fluid can be described as a function of the external magnetic field applied to it. With the application of a field, the dipole moment of the paramagnetic particles tend to align to the field, although this effect is partially counteracted by the thermal energy [21]. The fluid saturates when presented with a high external field. The saturation value is linearly related to the particle concentration.

2.1.1 Magnetoreological fluids vs. Ferrofluidic fluids

A distinction can be made between two types of magnetic fluids: magnetorheological and ferrofluidic. The main difference defined in this thesis between the two fluids is on the colloidal stability and particle size.

Magnetorheological fluid (MF) can be defined as having paramagnetic particle properties but lacking colloidal stability. This is because of the relatively large size of the particles in the range of $100 - 1000nm$. This increases the magnetization of the particle and its mass. These make the magnetic and gravitational energy larger than the thermal energy, creating instability. Coating of the particles is not always applied, adding to the instability when adding an external field. The particles aggregate and the fluid almost changes from a liquid to a solid. Ferrofluids (FF) on the other hand have paramagnetic particles with a size up to $10nm$ [19]. The smaller size, combined with almost always having a coating, results in colloidal stability. It is attracted by fields but will retain its liquid qualities.

In the remainder of this thesis, FF will be used as the magnetic fluid and all references to magnetic fluids will be towards this fluid. This is because of the properties that are specifically attributed to it.

2.2 Ferrohydrodynamics

Several hydrodynamic phenomena occur in a shaft assembly filled with liquids. With magnetic fluids more terms are added. In this section the instability of the FF seal in a dynamic situation will be analysed as well as the concept of fluid pressure build-up with an external field.

2.2.1 Instability

A FF seal that needs to seal against water has an interface at which the fluids touch. For simplifications, the interface is presented as a 2D linear interface in figure 2.1a [22]. Flow is in the x-direction and the two fluids move relative to each other. For $z > 0$ the velocity is U_1, density ρ_1 and magnetic permeability of μ_1, while for $z < 0$ the velocity is U_2, density ρ_2 and magnetic permeability of μ_1. When the interface becomes unstable, it starts forming a wave pattern as can be seen in 2.1b.

To find out the interaction between these two moving bodies an analytical instability equation is needed.The Kelvin-Helmholtz instability predicts the behaviour of a plane interface between two moving fluid layers. Considering the layers to be very thick, a simplified version of the dispersion relation becomes [23]

$$\omega = \frac{k(U_1\rho_1 + U_2\rho_2)}{\rho_1 + \rho_2} \pm \frac{k}{(\rho_1 + \rho_2)^{1/2}}\beta_k^{1/2} \tag{2.1}$$

where

$$\beta_k = \frac{g(\rho_2 - \rho_1)}{k} + k\sigma + \frac{(\mu_1 - \mu_2)^2 H_x^2}{\mu_1 - \mu_2} - \frac{\rho_1\rho_2(U_2 - U_1)^2}{\rho_1 + \rho 2} \tag{2.2}$$

In the equation k is the wave number, σ is the surface tension between two surfaces and H_x is the magnetic intensity at the interface parallel to the x-axis. The flow is stable as long

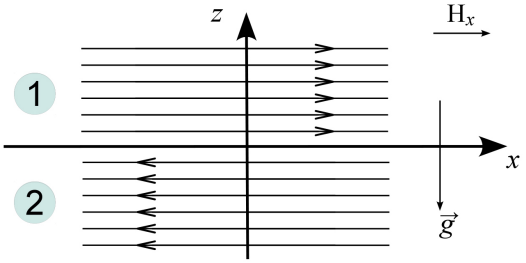

(a) The velocity profile of the two fluids are shown, as well as the direction of the magnetic field and gravity. Figure modified from [22].

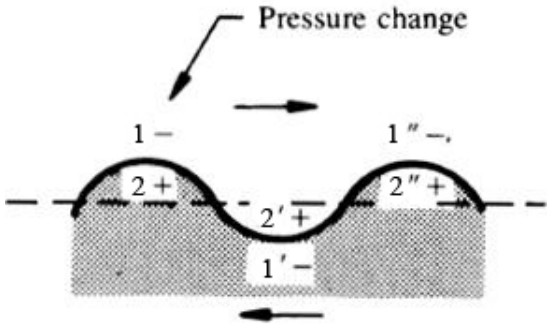

(b) The instabilty that arises is shown. Differences in speed create waves caused by local changing of the pressures in the fluids. Figure modified from [23]

Figure 2.1: Illustrations of a two fluid interface with a relative velocity difference.

as $\beta_k > 0$. Rosensweig rewrites the equation to obtain the criterion for the Kelvin-Helmholtz instability with magnetic fluids

$$(U_2 - U_1)^2 > \frac{\rho_1 + \rho_2}{\rho_1 \rho_2}\left\{[2g(\rho_2 - \rho_1)\sigma]^{1/2} + \frac{\mu_1 - \mu_2}{(\mu_1 + \mu_2)^2}(H^2)\right\} \tag{2.3}$$

In the model of figure 2.1a the two fluids are on top of each other and moving relative to each other. For (2.3) it is necessary that $\rho_1 < \rho_2$. Otherwise the fluid will start flowing towards the bottom due to the gravitational force. The velocity U_s of the fluid at the shaft boundary r, which in the shaft radius in meters, is called the *peripheral velocity* and is determined by the shaft's rotational frequency n given in RPM. The flow pattern is assumed to be a *Couette flow*

$$U_s = \frac{\pi n r}{30} \tag{2.4}$$

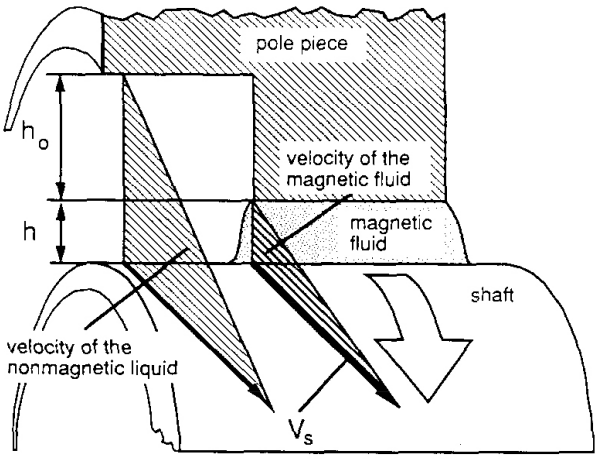

Figure 2.2: Illustration of a basic seal where there is a step in geometry at the interface. Figure taken from [1].

The relative velocity difference between the fluids mainly result from the geometry of the seal. It is common for seal designs to have steps in the outer housing or on the shaft, often

at the interface of the two fluids. This results in the difference in velocity gradient between the fluids (figure 2.2). The gradientis a function the height or gap size, measured from the shaft.

$$U_1 - U_2 = U_{\text{diff}} = \frac{h_0}{h_0 + h} U_s \tag{2.5}$$

2.2.2 Pressure build-up

For the design of the FF seal, it is important to have an idea of the amount of pressure the seal can withstand before leaking. An analytical model can give a quick insight into the seal's geometrical parameters of the seal, as well as its magnetic properties. The properties of pressure build-up can be divided into the *static case* and the *dynamic case*. From the static case it is possible to derive an analytical equation. The dynamic case has several factors that influence the pressure build-up and will be limited to empirical observations mentioned later in chapter 4.

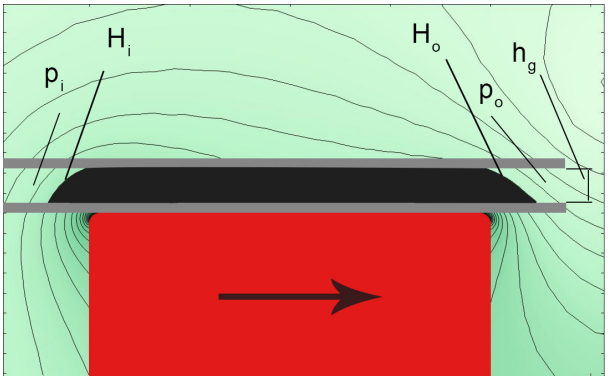

Figure 2.3: Illustration of a basic seal where the FF is sealing a small annulus. The FF interface with the air is parralel to the magnetic iso-lines depicted.

For the static case, the seal can be simplified to a 2D model, as seen in figure 2.3 of a cube magnet with a base plate and a top plate, where the FF seals the gap between magnet and top plate. One side is subjugated to a pressure increase (p_i) while the other side stays at ambient pressure(p_o). The gapsize (h_g) is the distance between the two plates. H_i depicts the magnetic strength at the interface parallel to the magnetic field lines on the high pressure side and H_o depicts that at the ambient pressure side. The prescribed pressure difference presses the FF outwards to the ambient side. Lampaert [17] used this model to demonstrate that the drop in pressure is correlated to the magnetic isolines on which the FF interface is located and formulated an equation for this for 3D seals.

To derive the pressure difference in the static case the Navier-Stokes equation is taken.

$$\rho \frac{\partial u}{\partial t} + \rho u \cdot \nabla u = -\nabla p + \eta \nabla^2 u + \mu_0 M \nabla H + f \tag{2.6}$$

Based on [17] the velocity component u and all other body forces, except for the magnetic body force, will be neglected

$$\nabla p = \mu_0 M \nabla H \tag{2.7}$$

where μ_1 is the magnetic permeability of vacuum, M is the saturation magnetization strength and ∇H is de magnetic intensity gradient. To find the pressure across the seal the equation can be written out as follows

$$p_i - p_o = \int_C \nabla p \cdot dl = \mu_0 M_s \int_C \nabla H \cdot dl = \mu_0 M_s (H_i - H_o) \tag{2.8}$$

where l is the thickness of the magnet, the integral is circular and H_i and H_o are the magnetic intensities at the interfaces on either side of the seal. This equation is only valid for if the magnetization strength is saturated (M_s). The equation shows that the static case pressure difference is only depended on the intensity at the interfaces.

Chapter 3

Principles of a FF seal design

In the process of designing a FF seal, it is essential to have an in-depth knowledge of the basics of contemporary FF seals in order to understand where improvements can be realised. This chapter will look at the geometric principles of the seal components as well as the engineering knowledge coupled with the overall concept. This includes the application of the magnet, creating the *liquid o-ring* and its general application.

The scope of this thesis stated that sealing with FF's seals for rotating shafts given the advantages this has over conventional seals is of interest. A FF seal operates as a contactless seal, meaning that no part that directly completes the sealing capability by mechanical contact. This severely reduces the wear on components and drastically improves the lifetime, based on maintenance and component replacement. The focus of maintenance then shifts from shaft and mechanical deterioration to the FF where loss of fluid and degradation become important issues. Another advantage lies in the fact that when the o-ring is breached by overpressure, the seal reforms and maintains its properties, making it compliant to sudden changes in operational conditions. Howerver, the seal will fail if the sudden pressure change is too great, resulting in the expulsion of FF from the seal, called a *blow out*. The system FF seal can be divided into several principle subsystems, from which any design can be generated.

3.1 Magnetic field generation

Magnets are used as the source of the magnetic field. The direction of the field and that its homogeneous nature around the shaft is important. The magnetic field direction here is axially. This means a single seal can consist of a single ring magnet or multiple magnets configured in a ring around the shaft. The functionality does not necessarily require a specific magnet geometry, as long as the prescribed magnetic field configuration and direction are kept. The image on the left in figure 3.1 demonstrates the sealing principle of a single ring magnet around a shaft. This is a cutthrough of the seal with only the top side visible because of symmetry.

3.2 Magnetic field guidance

To create the seal at the shaft, the fields have to be guided towards the shaft. A simple method to achieve this is to directly place the magnet close to the shaft as seen in the left figure of 3.1. No magnetic conducting material is used and furthermore, the shaft cannot conduct the field lines. This can be specifically advantageous when using ring magnets, specifically for small diameter shafts. Disadvantages are the increasing costs for large shaft diameters. An other method is to guide the field lines towards the shaft using *pole pieces*, made from material with a high magnetic permeability. The picture on the right in figure 3.1 shows the guidance of field lines. To complete the magnetic circuit the shaft also needs to have a high

magnetic permeability or have a sleeve to function as the magnetic conductor. This increases the pressure build-up in the FF seal [24]. By having a closed circuit with this method the seal is less susceptible to external disturbances such as those resulting from other magnetizable metals in the vicinity.

Figure 3.1: Basic concept of a seal. The FF between the magnet and the shaft (left) creates a liquid o-ring that forms around a non-magnetizable shaft. For engineering purposes pole pieces can be added (right) to facilitate or improve the sealing capacity. The shaft has to be magnetically conducting for this method.

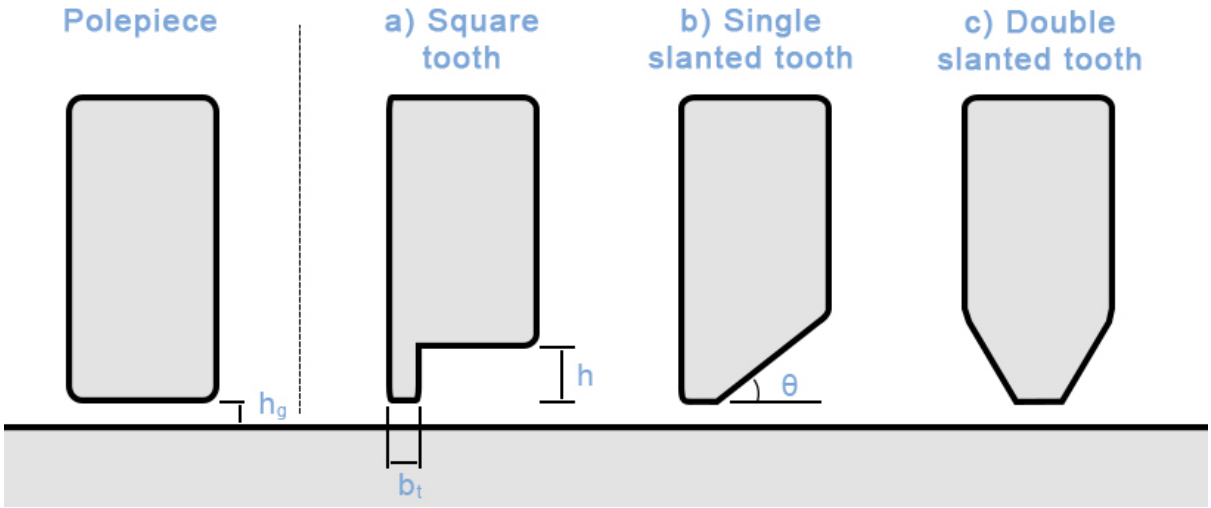

Figure 3.2: These are some basic geometries that can be used. The horizontal dotted line is the symmetry line of the seal. The teeth can improve the seal by concentrating magnetic field lines or by creating a better FF containment.

3.3 Magnetic field convergence

At the end of a pole piece a *tooth* can be added to improve the magnetic flux near the shaft. By altering the geometry near the shaft the field density can be improved. Important parameters are the distance between the tooth and shaft h_g (gap size), width of the tooth b_t, lenght of the tooth h and use of slanted edges θ. Figure 3.2 shows a few basic geometries that be designed. Because the shaft is also magnetically conducting, it is also possible to have the tooth on the shaft. By placing several teeth on the pole piece the number of sealing rings per magnet configuration can expanded. This initially increases the sealing capacity linearly and levels off after a certain amount [4]. When adding multiple teeth on a pole piece the distance between

the teeth b becomes an added parameter. Figure 3.3 illustrates such a seal. An other method of increasing the number of seals is by using multiple magnet configurations in series. The distance between the magnet configurations or pole pieces are again an important parameter.

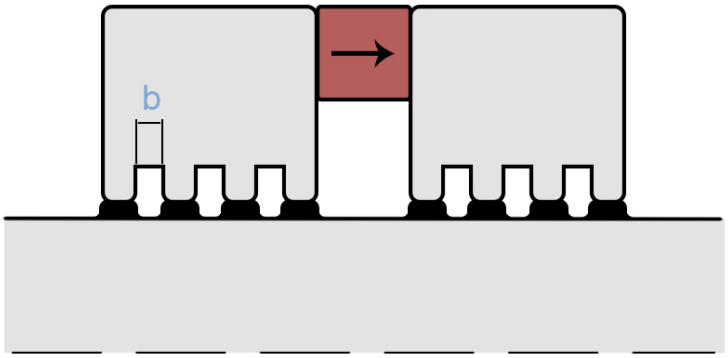

Figure 3.3: This is an example of a pole piece seal with multiple teeth. the field lines are concentrated through these teeth. Having the seal symmetrical can double the capacity of the seal.

3.4 FF seal

The FF will form a liquid o-ring of FF between the magnet configuration or pole piece and the shaft to which it can hold a certain pressure difference. The amount of FF needed is typically set to between 1.5 and 3 times the nominal gap volume [5]. Having several seals in series, as demonstrated in figure 3.3, increases the total pressure difference a seal can withstand. The pressure will distribute over the seals by inter seal leakage until all inter seal cavities have been pressurised. The design can now withstand higher pressures in comparison to a single seal.

Chapter 4

Ferrofluidic seals in literature

The first commercial applications of FF seals can be traced back to the ’70 [25]. These seals were designed to be used in systems with pressure difference of several bars or high vacuum of 10-8 Torr. Since then the number of patents and research on the system has steadily increased over the years and their application has expanded.

The focus of this chapter will be to discuss several publications where a FF rotational seal is used. The publications will be broken down into subjects of theoretical application, test parameters and testing methods. The aim will be both to insight on the state-of-the-art of the technology and also to identify gaps in the existing technology.

4.1 Ferrofluidic pressure seals

This section contains a selection of papers concerning FF seals for sealing gasses or vacuums. The selection is based on works that are specified on their relevance to the scope of this thesis or hold interesting test results. The publications have been arranged chronologically.

4.1.1 Magnetic Fluid Seals for Special Applications [1980]

This paper on FF seals is by K. Raj et. al. [2]. They looked at three different applications for a FF seal. These are: a belt edge seal to contain dangerous gasses over a large surface (fig. 4.1), a large shaft diameter seal (12 cm) to hold large pressure differences and a centrifugal seal for use in high-speed shaft systems (>3000 RPM). The performances were researched based on the dependency on viscosity, temperature and power loss.

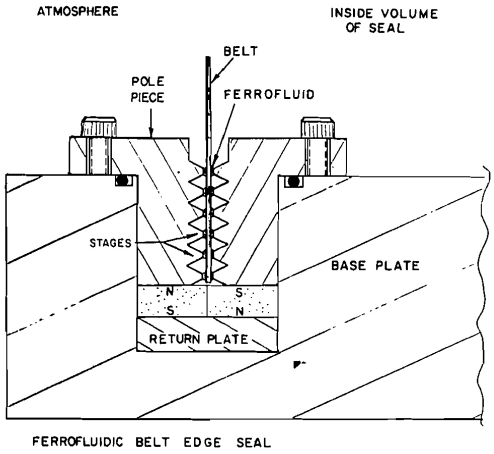

Figure 4.1: This side view illustrates the concept of the belt edge seal.The nonmagnetic belt is sealed on two sides. Figure taken from [2]

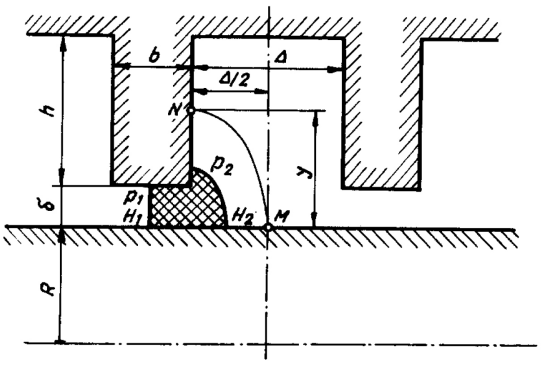

Figure 4.2: A sketch of the seal gap geometry. Figure taken from [3]

4.1.2 Magnetic fluid seals: Some design problems and applications [1987]

This publication by I. Anton et al [3] shows fundamental work on the geometry of the seal design. They simplified the teeth to rectangular shapes to find analytical relationships. Figure 4.2 shows the parameters like shaft radius, gap size, teeth width and saturation that have been considered. A theoretical optimum was found between the tooth width and gap size. The paper mainly focusses on vacuum application.

4.1.3 Numerical Calculations for Ferrofluid Seals [1992]

This work by Zou Jibin et al [4] checked the sealing capacity when the number of teeth, tooth width, teeth spacing, gap size and the amount of FF is varied while having a constant magnetic intensity. They compared their findings with analytical models, suggesting that the maximum pressure difference can be calculated and a optimal tooth configuration (fig. 4.3) can be designed.

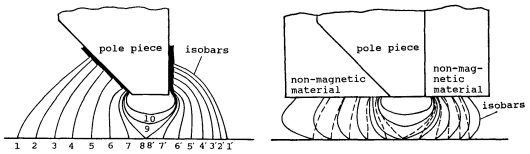

Figure 4.3: Sketch of the isobars around the pole. The left one is in static case. The right one is for the dynamic case where nonmagnetic "stuffing" has been used to reduce the effects of centrifugal forces. Figure taken from [4]

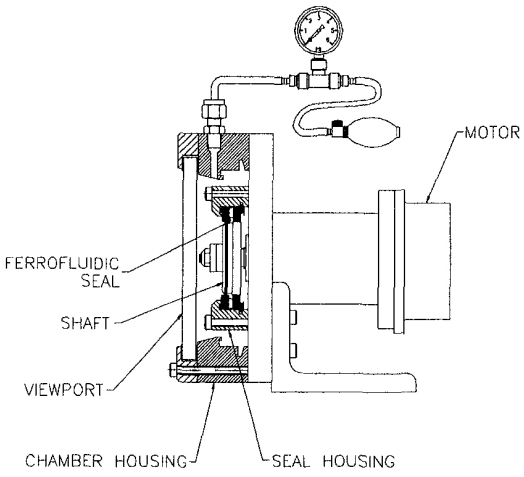

Figure 4.4: The full setup with the diameter of the shaft and the position of the tooth. A pressure chamber has been built around it. Figure taken from [5].

4.1.4 Experimental Study of High Speed Sealing Capability of Single Stage Ferrofluidic Seals [1997]

A study on very high rotational speeds up to 55 kRPM (peripheral speeds up to 293 m/s) was performed by J Bonvouloir [5]. The setup in figure 4.4 could hold different shaft diameter between 25.4 and 101.6 mm and tested different tooth configurations (on the shaft or on the pole piece). Tests were performed on burst pressure, varying shaft speed and type of FF. Also eccentricity of the shaft was evaluated. The paper shows that at low speeds a tooth on the shaft provides for a better result, but for higher speeds, this is the case when placing a tooth on the pole piece which also handles eccentricity better.

4.1.5 New designs of magnetic fluid exclusion seals for rolling bearings [2005]

This paper by W. Ochonski [6] shows a lot of innovative designs for FF seals. These seals are called *exclusion seals* for their application in ultra clean environments where particles and moister need to be excluded from machinery. The seals all have iterations on the pole piece geometry. There are some patents shown, suggesting that these can be used in industry. This paper is mainly useful when looking at new ways to use the pole piece in the seal. Figure 4.5 shows an example of an exclusion seal.

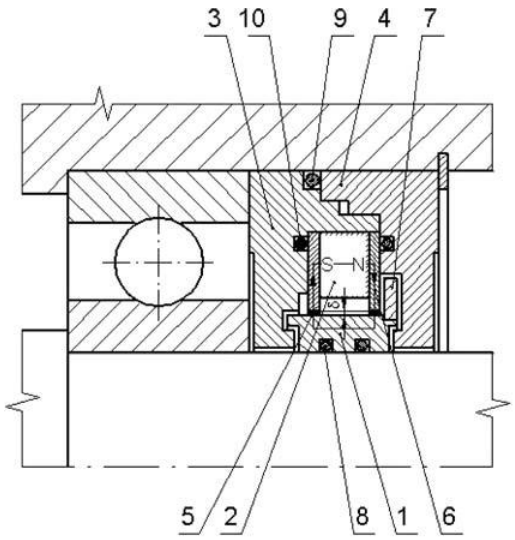

Key
1 – rotating sleeve; 2 – permanent magnet; 3, 4 – elements of seal casing; 5 – magnetic fluid; 6 – pole pieces; 7 – shield; 8, 9, 10 – "O"-ring seals

Figure 4.5: An example of an exclusion seal. It is composed of a magnetic fluid seal and a greased labyrinth seal. Figure taken from [6].

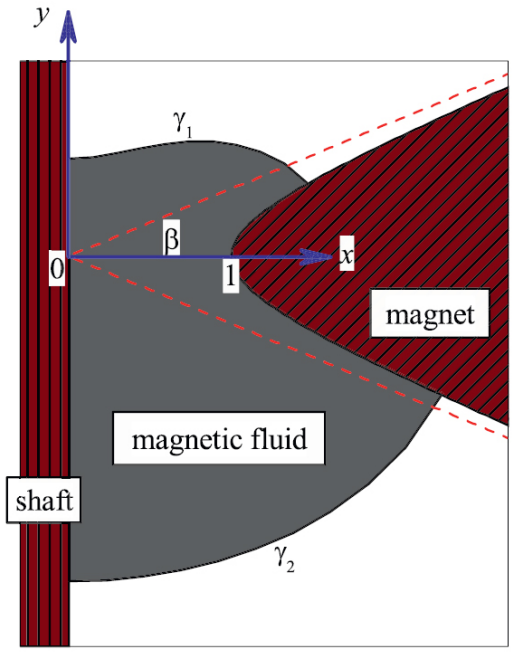

Figure 4.6: Illustration to the problem statement: $\gamma 1$ and $\gamma 2$ are the free surface on the high and low pressure region, respectively. The dashed lines show the asymptotes to the concentrator hyperbola and β is the half-angle between the asymptotes. Figure taken from [7]

4.1.6 Influence of diffusion of magnetic particles on stability of a static magnetic fluid seal under the action of external pressure drop [2011]

V. Polevikov et al. [7] did a thorough study on the static case. They present a mathematical model to study the stability of the FF seal. Their focus lies in the effect of the FF particle diffusion on the stability of the seal, which has been assumed or neglected in previous research. The model is based on equations of Navier-Stokes, Maxwell, Langevin and Young Laplace among others, to create the magnetic isolines. The model is visualised in figure 4.6. Their work states that there is a non-neglectable influence of the particle diffusion from the fluid towards the polepiece on the critical pressure. Over time and with increasing the amount of FF the critical pressure improves due to the dense packing of particles.

4.1.7 Study on Magnetic Fluid Static Seal of Large Gap [2012]

According to Li Decai [26], most previous publication have only worked with small shaft diameters (in the range of 15 - 50 mm) or small gap sizes (smaller than 1 mm). This study considers shafts with considerable larger diameters and seal gaps. A shaft of 300 mm and a gap sizes larger than 1 mm have been used for the research. It Concludes that increasing the gap size has a negative effect on the stability, whereas increasing the amount of FF, entails a higher saturation magnetization of the FF and prevents temperature increases, thus has a positive effect.

4.1.8 Experimental and numerical determination of the static critical pressure in ferrofluid seals [2013]

In this paper an analytical FEM model was created by W. Horak, together with M. Szczech [8], as a prediction method on the burst pressure in a FF seal in the static case. In their experiments they varied the gap size and the amount of FF used. Their focus remained on static situations.Figure 4.7 shows a sketch of the setup. They varied the gap size and the amount of FF used. The error between their model and experiments varied between -1.4 and -34.3%.

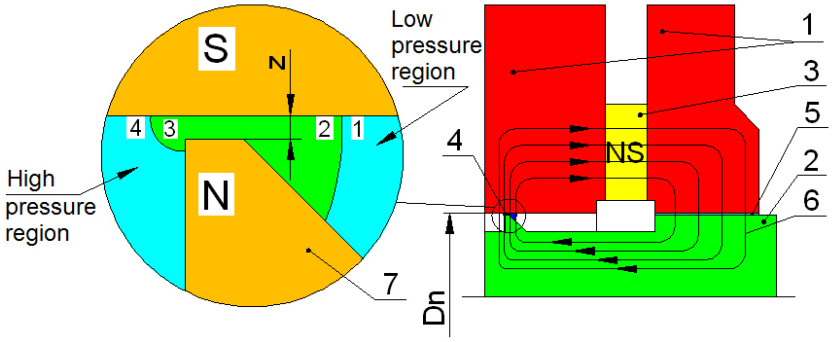

Figure 4.7: Illustration of the magnetic field lines and geometry of the tooth. Figure taken from [8].

4.2 Ferrofluidic pressure seals for liquid/liquid interface

One of the main disadvantages given by [25] is that FF should not be used in sealing liquids, for the seal can easily be washed away. However, there have been numerous publication concerning a liquid/liquid interface indicating how to prolong the life expectancy of the FF seal. Concepts such as shields, water insoluble FF's and fluid instability reduction will be discussed in the following section.

The publications have been selected based on their relevance to the scope of this thesis or of is they hold interesting test results. The publications have been arranged chronologically.

4.2.1 Some experiences using a ferrofluid seal against liquid [1980]

Since the first experiments done on FF seals, research was done on using FF seals for sealing liquids. This early paper by R. Wiliams et. al. [9] considered testing miniature multi stage seal at low rotational speeds (0.0006 m/s) against air, water and fluorocarbon liquid coolant. A sketch of the set up is displayed in figure 4.8. Testing the set-up for 6 consecutive days at a sub critical pressure showed no noticeable difference on the performance of the seal.

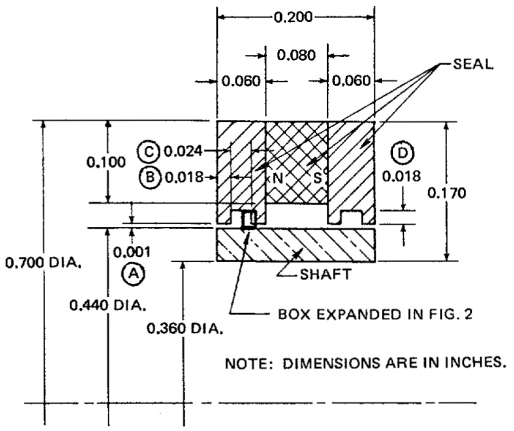

Figure 4.8: Sketch of the seal configuration. Figure taken from [9]

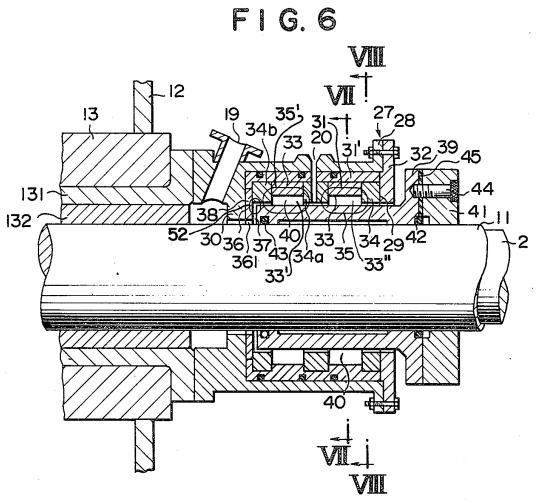

Figure 4.9: Design of the patent by Tamama et al. with a sleeve. Number 20 indicates the inlet for the FF, 19 the inlet for clean sea water, 132 the lignumvitae and 36 the magnetic rubber disk.

4.2.2 Device for sealing a propeller shaft against invasion of water [1984]

Patent by Tamama et al.[27] on a basic FF seal design, for use in ships against seawater. Interestingly the patent also shows the basics of conventional seals. The design in figure 4.9 contains a lignumvitae, a wooden part used as shaft bearing or stern tube. Sea water is pumped between the stern tube and the seal as a method for protecting and lubricating the stern tube. The water is pumped from a location far away from the propeller to keep the water relatively clean. Next to the conventional pole pieces on the seal a rubber magnet disk sealing a radial gap further increases the sealing power. FF can be added though a supply hole in case of fluid loss, due to mixing with seawater.

4.2.3 Sealing liquids with magnetic liquids [1990]

This publication focusses on the deterioration of FF and the causes thereof. J. Kurfess et al [1] presents three set-ups: set-up 1 tests shielding of the magnetic seal against the non-magnetic liquid, set-up 2 shows a hollow glass shaft and a mirror allowing one to observe the liquid-to-liquid interface and set-up 3 tests FF deterioration by measuring the power consumption. Figure 4.10 contains illustrations of the first two setups. An important aspect of this paper is the earliest paper on FF seals found making reference to the Rosensweig inequality.

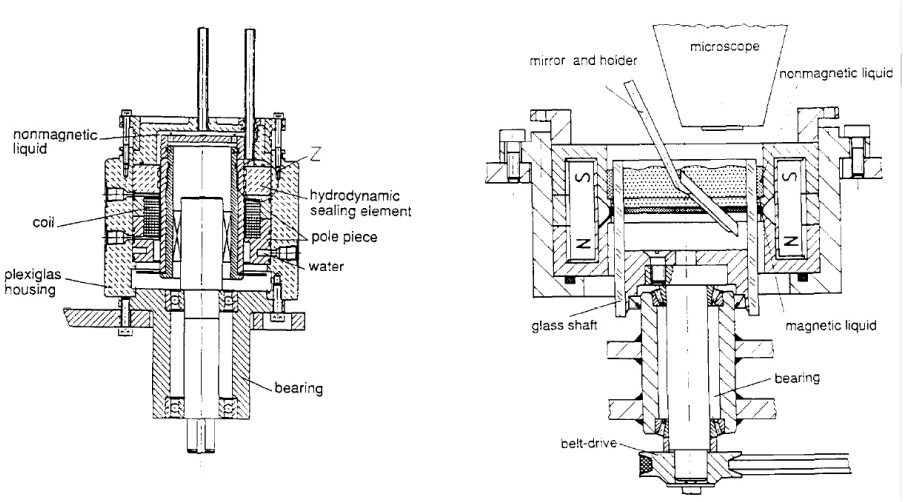

Figure 4.10: In the left setup it is possible to mount different sealing element. In the setup on the right it is possible to view the FF seal during testing. Figures taken from [1]

4.2.4 FF Seal for Rotary Blood Pumps [2001-13]

Yoshinori Mitamura has written several papers on liquid/liquid FF seal interfaces, in particular in sealing blood[28, 29, 30, 10, 11]. In collaboration with others he designed a seal which has a shield to prevent FF mixing with the blood. Figure 4.11 shows the full set up for testing the seal, while in figure 4.12 the illustration represents testing the seal in different configurations. After the first paper, where the sealing stability of 51 days for the dynamic case, the researchers have been able to improve this results to 275 days by synthesising their own FF, changing the geometry of their shield, through numerical analysis on fluid speed difference at the interface and FEM analysis of the fluid (blood) flow. Directly mixing FF with water and testing the properties over time, he claims that the magnetization of the FF deteriorates over time, meaning that the FF tested lose their sealing capacity when exposed to water.

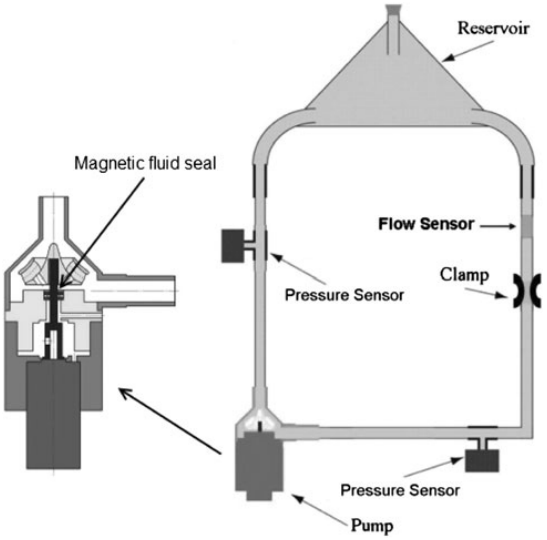

Figure 4.11: The full set up used in one of the experiments. Figure taken from [10]

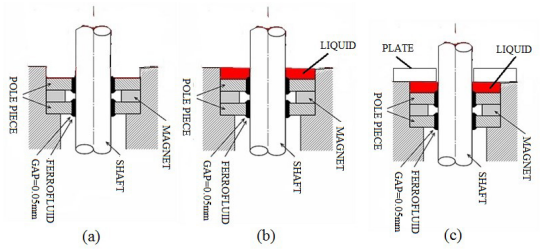

Figure 4.12: By altering the position of the seal and including a shield, improvements of the lifetime were observed. Figure taken from [11]

4.2.5 Design optimization of seal structure for sealing liquid by magnetic fluids [2005]

This publication by T. Lui [12] continues the work of [1], finding solutions to minimize the instability at the interface. A major problem is due to the fact that instability arises when, at the interface, there is a significant amount of magnetic leakage. This situation is improved by using soft iron bushing on the shaft. An other issue is the relative speed difference (Rosensweig). To minimize this difference a shield was added. The imposed improvements can be seen in figure 4.13. Through empirical testing the researchers found an optimal thickness for the bushing and the shield. The set up was able to run uninterruptedly for 10 weeks with a shaft diameter of 20 mm and a peripheral speed of 1,26 m/s and managed to hold a reservoir of oil and an added pressure difference of 3 kPa.

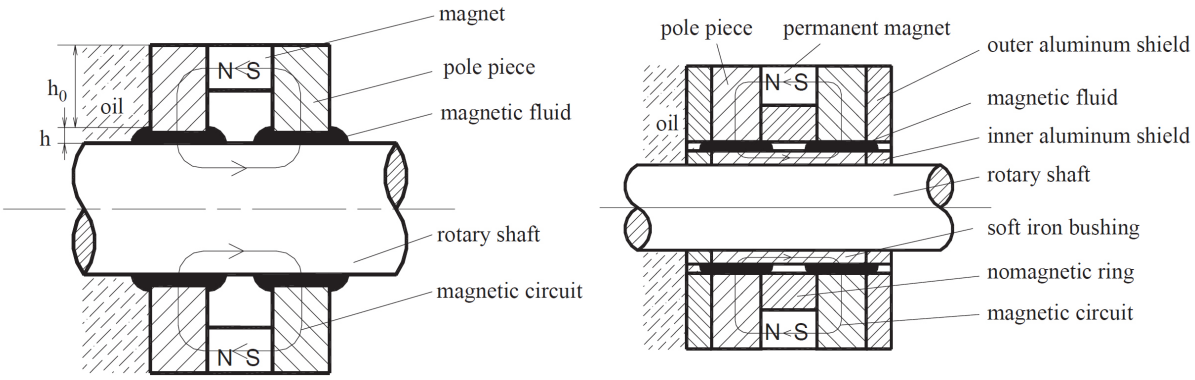

Figure 4.13: On the left the sketch shows a basic model of a FF seal. The right sketch shows the alterations intorduced by the author. Figures taken from [12]

4.2.6 Magnetic fluid seals for rotary shafts working in water [2007-13]

A great deal of research on FF seals in (sea)water have been performed by L. Matuszewski and colleges. He has published several papers [13, 31, 32, 14, 33] on the subject. His first set-up (figure 4.14) was realized in collaboration with Szydlo. Their findings suggested that, for certain sub critical speeds and pressures, the seals can have a long seal life (201 h). Shields proved to increase seal life, but also to increase the temperature in the FF. In later work, both of them concentrated on practical applications of the seal and they found that a FF seal should always be preceded by a conventional seal. They invested in a new set-up which could hold larger shaft diameters. From this moment onwards, they abandoned the concept of the shield. This allowed them to discovered that the magnets can lead to run-out (eccentricity) of the shaft. The first set-up was reused to perform tests with a single tooth on different commercially available FFs. This was followed by an in-depth research on the critical pressure and speed, as well as on the lifetime of the seal. In later works the duo split and Matuszewski repeated the experiment on a set-up of his own design(figure 4.15).

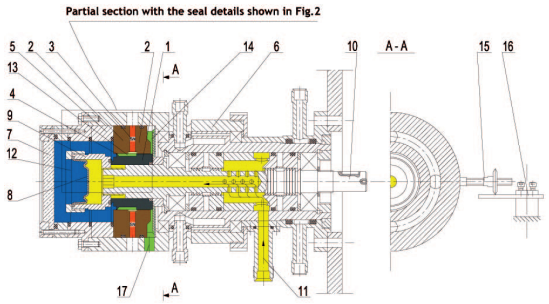

Figure 4.14: Detailed depiction of the setup designed by the duo. Figure taken from [13]

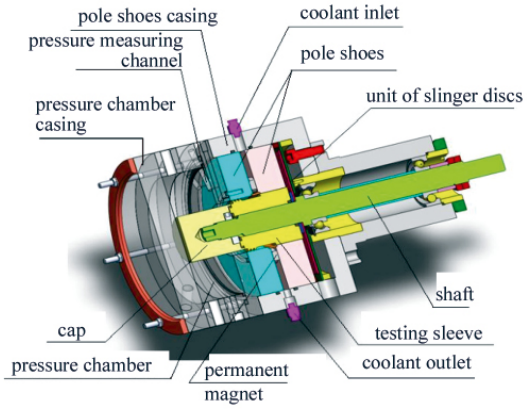

Figure 4.15: A re-iteration of the previous setup, designed by Matuszewski. Figure taken from [14]

4.2.7 Magnetic nanofluids and magnetic composite fluids in rotating seal systems [2010]

A study where the researchers T. BorbÃąth et al. developed themselves different FFs [15]. The paper shows designs for gas systems (high pressure and vacuum), as well for some other systems for liquid application. In the basic design, the researchers take in account magnetic flux dissipation. They also look at the effects of centrifugal forces and viscous heating, but claim this to be non-significant for peripheral shaft speeds in de range of 10 m/s. The liquid sealing shown in the design (figure 4.16) is for liquefied gasses and consists of a mechanical and a FF seal. The mechanical seal can hold 3 bars. The FF seal is only present to prevent gas that is leaking from the mechanical seal, which is at a much lower pressure, to leak into the environment. The gas can then safely be evacuated.

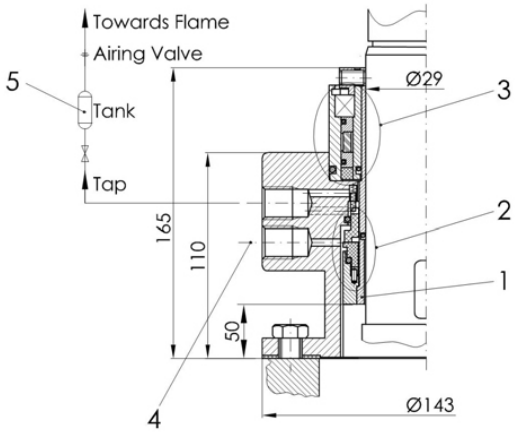

Figure 4.16: Sketch for the liquid gas hybrid seal. Figure taken from [15]

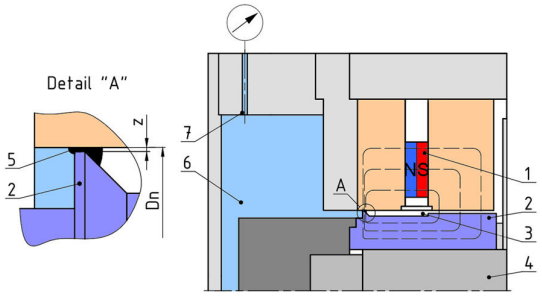

Figure 4.17: Similar to the previous set up by the duo, this test set up can hold and pressurize water. Figure taken from [16].

4.2.8 Tightness testing of rotary ferromagnetic fluid seal working in water environment [2015]

In this selection, the second paper by the duo Szczech and Horak [16], depicts l/l interfaces. This paper is a summation of most of the important works that have been discussed in previous papers. The researchers carry out simple burst tests with different FF's to find the critical pres-

sure. Figure 4.17 is an illustration of the mentioned setup. They also perform stepwise burst pressure experiments in the dynamic case. A novelty in this paper is that they use mathematical model to describe the critical pressure as function of the rotational speed, critical pressure and FF density. Lastly a durability test was performed to see what happens with a constant rotational speed and stepwise pressure increase to see how the pressure redistributes. From this experiment both concluded that there is some pressure loss between the step increases. According to them, this loss is caused by the peripheral speed of the seal, by the water pressure and by other properties of the FF such as dynamic viscosity, surface tension and saturation magnetization.

4.3 Conclusion

The literature shows that, when comparing sealing **gasses (or vacuums) and liquids**, the former have been successfully implemented into industry, where as the latter still remains in the research phase. The first type o seals can have a seal lifetime of several years, while the last type has only seen lifetimes of up to 275 days (in the cases where long duration tests have actually been performed). The critical pressure determines the maximum pressure that can be applied until failure but the mentioned seals fail at sub-critical pressures, entailing that there are certain phenomena that play a role there. Which leaves the question *Why does the seal leak?*

In the past, this question was tackled by improving the geometrical design of the seal. All the mentioned papers refer to the concept of pole pieces with magnetizable shaft. Here, the advantages are that the pieces are easily manufactured to fit the geometry of the shaft, can be made to very precise dimensions and, when crafted with highly magnetic permeable and saturation capacity material, the configuration of the magnets is less crucial. One advantage is that the seal is less vulnerable to external disturbance, like other magnetizable metals in the vicinity. Many design options have been realised for the FF seal to pinpoint the performance variables and optimize those variables. In the case of the pole pieces, they can mainly be attributed to the teeth of the seal. For a single tooth, this has been its geometry (length, width, angle(s)) and the gap size. With multiple teeth, the number of teeth, the tooth spacing and number of magnetic rings become important. These improvements create the optimal magnetic flux between the magnet and the shaft, resulting in a seal with a high pressure difference capacity. This high magnetic flux can also be created by placing the magnet close to the shaft. It is an alternative for smaller shafts, where ring magnets are readily available. An alternative method for improving the sealing capacity was to find FFs that better suit the requirements of the seal. Increasing the saturation improves the pressure drop that the seal can handle. The study of RosensweigâĂŹs fluid interface instability, discussed in chapter 2, led to improving the seal design, one of the enhancements was the use of shields, which limit the speed difference between the fluids at the interface. The other one was to reduce the interface contact surface.

These methods have helped to increase the lifetime of the l/l, yet there is still leakage. The answer then probably lies with the **magnetization deterioration of the FF** [29]. The fluid loses its pressure build-up characteristics when exposed for a prolonged time to water and it is suspected that the carrier is deteriorating. If this is the case, a solution could be to remove the 'depleted' FF from the seal and to replenish it before the seal starts to leak. In the next chapter, a new FF seal concept will be introduced that uses this method of FF replenishing.

Chapter 5

Passive transport of Ferrofluid in a liquid contactless seal

Contactless FF seals have been around for some time and have commercial success for sealing gasses and vacuums. With the use for sealing liquids, the seals lifetime tends to be too short for commercial use. This is due to the fact that, in contact with water, the FF deteriorates over time. This paper presents a solution for increasing the lifetime of the seal by replacing the deteriorated fluid during use, without losing its sealing capacity. This result is achieved by pumping fresh FF into the first seal and by using the attracting magnetic force of subsequent magnets to transport excess fluid to the last seal, where it can be removed or recycled. A FEM model of the seal was created to predict the pressure drop of the set-up. The experiment shows a critical pressure corresponding with the model and the fluid transport happens without pressure loss at the inlet chamber. The result show that a seal using this concept has great potential in increasing the lifetime of FF seals.

5.1 Introduction

The sealing technology for moving parts, like rotary shafts using ferrofluids, dates back to the '70 [25]. Ferrofluids (FF) are a colloidal stable suspension of very small magnetic particles ($\sim 10nm$) in a carrier, giving the fluid paramagnetic properties. When a magnet is mounted radially around a shaft and FF is added in the gap between the shaft and the magnet, the internal pressure builds up in the fluid and creates a contact-less seal capable of withstanding an external pressure difference over the seal. The geometry of the seal can be adjusted to improve the pressure drop capacity by changing, among other things, the gapsize, the number of sealing elements, magnet strength and the magnetic saturation of the FF. The seal is capable of withstanding pressures from gasses, as well as high vacuums [25] and are commercially available. FF seals have also branched out to sealing liquefied gasses and other liquids like water, although their commercial success is still lacking.

The main issue of the FF seal in an aqueous environment is the inevitable leaking due to the deterioration of the FF [29]. Even if the seal has been correctly designed, the sealing capacity eventually degrades through interaction with water (by direct contact and mixing), to the point that the seal starts to leak or fail all together. Methods to limit the direct contact and to prevent mixing have had significant results [1] [29] [12] [32] in increasing the lifetime of the seal, but still did not prevent degradation.

This paper presents a method for increasing the seal's lifetime by removing degraded FF at the water interface. This is done by pumping fresh FF at the interface and draining the older FF by passive transport via the subsequent seals. In doing so, the lifetime is no longer dependent on the state of the FF.

5.2 Method

The basicfunction of a FF seal is to form a liquid barrier in a thin gap or annulus, often between a magnet or pole piece [3] [chapter 3] and a shaft. To simplify the conditions and fabrication for testing FF transport a stationary channel has been chosen.

The seal is defined as the assembly of magnets with FF sealing elements. A single element is defined as a liquid barrier over which a certain pressure difference can be hold. For a single magnet in the channel the sealing element is formed as shown in figure 5.1, where the interface between FF and the air are parallel to the magnetic field lines [4]. Exercising a pressure on one side shifts the seal toward the lower pressure side until a pressure equilibrium has been obtained. If the pressure becomes too high it exceeds the maximum internal pressure in the FF and the seal leaks. This is called the critical pressure p_c. If the gap size is small enough, two sealing elements can form, trapping a pressure between them. By adding multiple seals p_c can be increased, where each seal contributes to sealing a part of the total pressure.

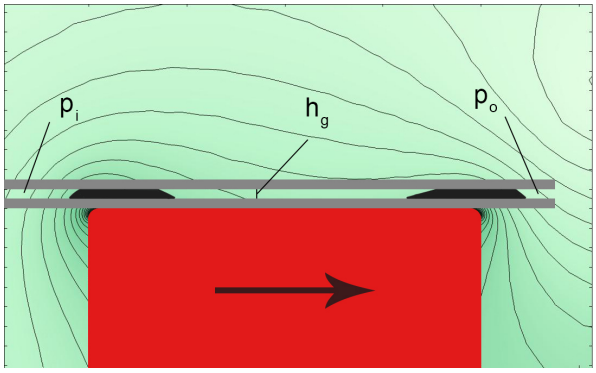

Figure 5.1: Representation of a cutthrough view of a sealing element. Magnet is shown in red and the arrow indicates magnetization direction.

In the degradation of FF the only part of the seal that is affected is at the water interface. Removing this fluid and replenishing it with fresh FF without leakage is therefore of importance. In the following method the failure of a seal will be attributed to the leaking of the first sealing element.

5.2.1 Concept

The transport of FF works by the addition of FF at the first sealing element under pressure. The addition leads to a volume increase of FF in the channel moving the FF interface to the point that the magnetic field of the neighbouring magnet is stronger, creating a flow of FF towards the other magnet. The movement of FF creates a cascade effect moving surplus FF from one magnet to the other towards the exit of the setup. The process has been illustrated in figure 5.2.

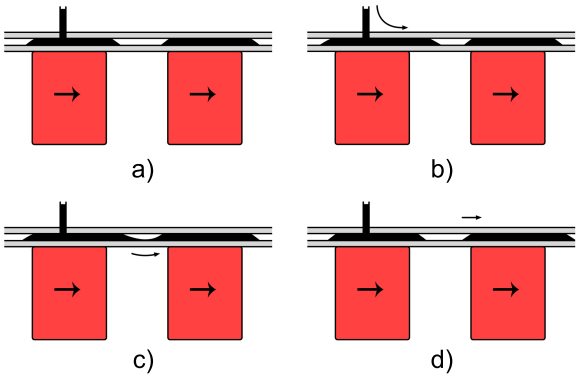

Figure 5.2: Transport of FF. The seal is first a) at equilibruim. Then FF is added b) to the first sealing element, moving the interface. Magnetic forces c) of the second magnet become more prevalent on the fluid, pulling excess towards it. Finally equilibrium restores d) with the excess fluid now on the second magnet.

The inner pressure p_i in figure 5.1 represents the pressure the seal needs to withstand. The outer pressure p_o is the ambient pressure. The pressure in the FF reservoir is denoted by p_{FF}. Between each seal, a pressure chamber is created denoted by $p_{i,n}$, where n is the n^{th} chamber in the seal. The chambers spread the pressure gradient over the sealing elements. The maximum pressure in each chamber is determined by the p_c of the sealing element holding its pressure. Increasing the pressure forces air past the seal element into the following chamber. Once all chambers are filled to their maximum pressure, the seal as a whole leaks.

To add FF to the system, the fluid is forced from a reservoir into the seal. The pressure needed to fill the sealing element depends on

where the fluid is added. Conceptual choices are 1) Adding FF on the lower pressure side of the element and letting the magnetic forces pull the FF back into the seal, 2) Adding FF on the inside of the element, close to sealing pressure and 3) Adding FF on the front end of the element, slightly above the sealing pressure and letting the FF flow into the seal as a result of magnetic forces and pressure.

For this experiment, having the FF inlet on the inside of the sealing element will be beneficial for mixing. Furthermore, the addition pressure is easy to attain. In order to get to this result, the pressure needs to be larger than the pressure in the first inner chamber pressure, but lower than the inner pressure to prevent leakage into the inlet chamber.

$$p_{i,s} > p_{FF} > p_{i,I} \tag{5.1}$$

5.2.2 Theroretical model

A model of the seal is produced to predict the pressure holding capabilities. For this the critical pressure is to be determined. The pressure drop of a single magnet is calculated using a modified version of the Navier-Stokes equation with an added magnetic component. The gradient of the pressure becomes

$$\nabla p = \mu_0 M_s \nabla H \tag{5.2}$$

where μ_0 is the permeability of air and M_s is the saturation magnetization of the FF. For a single magnet and a specific FF, equation (5.2) shows that the pressure gradient over a single seal is only dependent on the gradient of the magnetic intensity H. When the gradient of the pressure is defined as the pressure difference between both interfaces of the seal, the equation becomes

$$\begin{aligned} p_i - p_o &= \int_C \nabla p \cdot dl = \mu_0 M_s \int_C \nabla H \cdot dl \\ &= \mu_0 M_s (H_i - H_o) \end{aligned} \tag{5.3}$$

where H_i is the intensity at the higher pressure side of the seal and H_o at the lower pressure side. Expanding the pressure difference capacity over multiple seals is a summation of the magnets in series. The equation becomes

$$p_i - p_o = \mu_0 M_s (\sum_{i=1}^{n} H_{\mathrm{i},i} - H_{\mathrm{o},i}) \tag{5.4}$$

5.2.3 Comsol model

In order to find the magnetization gradient a FEM model is devised. Figure 5.3 is a 2D model that represents a cutthrough of the demonstrator. With the magnetic iso-lines, it shows the high gradient near the edges of the magnet and a low point in between the magnets. A total of 5 magnets with thickness $b = 4mm$ are modelled with a flux density of 1.22 Tesla and have the same orientation. Table 5.1 shows the parameters used for this model.

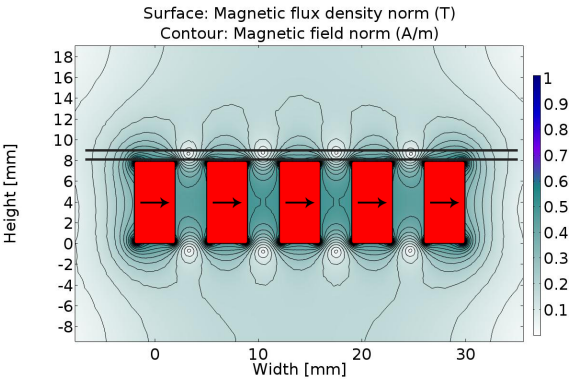

Figure 5.3: Magnetic field lines of the 2D model. The magnets are in red and the two horizontal lines represent the top and bottom of the channel.

Table 5.1: FEM model parameters

Br	1.22 T
orientation	x, same direction
nr of magnets	5
b	4 mm
d	3 mm

The pressure drop is defined at the locations of the interface of the FF. The theoretical highest pressure drop has a seal interface H_i at the highest H in the channel that is the furthest away form the magnet, which is the top surface of the channel, with H_o side's interface of the seal at the lowest H nearest to the magnet, i.e. the bottom surface of the

channel. This is because, at the higher pressure side it is the weakest point in the seal and at the lower pressure side it is the point at which FF will leak towards the next magnet. Figure 5.5 shows the magnetic field intensity at the top and bottom of the channel. The maximum difference in H can now be determined. Table 5.2 shows the local maxima and corresponding minima to be used for pressure drop calculation taken from figure 5.5. It is assumed that there is one sealing element per magnet. Two elements will produce a slightly higher pressure difference, but this is negligible. Using equation (5.4) and choosing for $\mu_0 = 4\pi \times 10^{-7} H/m$ and $M_s = 3.5e^4 A/m$ the pressure drops per seal are calculated in table 5.2.

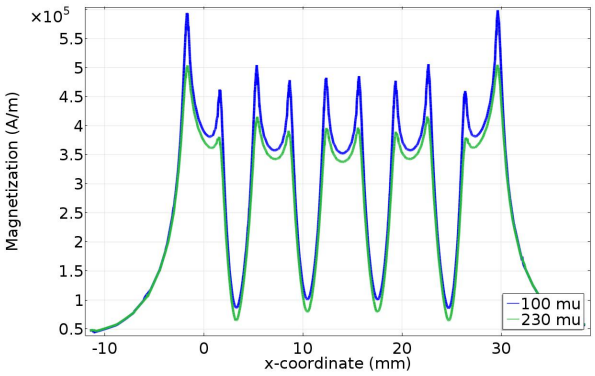

Figure 5.4: This graph shows the magnetization at the top and bottom surface of the channel. The upper surface corresponds to the height, measured from the top surface of the magnets, of 230 μm and the lower surface of 100 μm.

Table 5.2: Magnetization values from the FEM model for calculating the theoretical maximum pressure

Seal	$H_i * 10^5$ [A/m]	$H_o * 10^5$ [A/m]	Δp [bar]
1	5.13	0.87	0.19
2	4.10	1.02	0.14
3	3.92	1.02	0.13
4	4.18	0.86	0.15
5	4.71	0.00	0.21

Summation of the pressures gives a critical pressure of 0.82 bar.

3D model

A 3D model of the magnets has been added to further the analysis of the demonstrator . The average of a surface is taken to compensate for the variation in the magnetization due to mesh size. Figure 5.5 shows the average at the respective heights of 100 and 230 μm. Utilizing the same method, the pressure drop in this model is 0.53 bar.

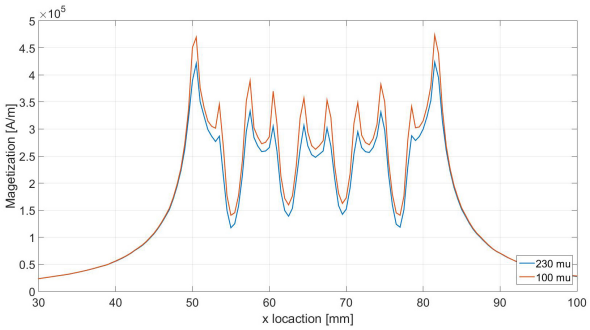

Figure 5.5: This graph shows the average magnetization at the top and bottom surface of the channel. The same height of $230\mu m$ and $100\mu m$ has been used.

Model correction

The result from the two models are assuming a perfect distribution of the FF, but also a perfect distribution of the medium separating the sealing element. If there is not enough air between the element or enough FF in the element, the interfaces can never be at the optimal position and thus the actual critical pressure becomes lower. Here, the design of the demonstrator can have a severe influence on this. Due to the small gap size, capillary effects become prominent. This results in FF transporting to the following seal via the side wall of the channel, decreasing the amount of FF in the seal and, consequently, decreasing the pressure difference. The distance between the magnets adds to this effect. The closer the magnets are to each other the easier it is to transport FF by capillary effect . Photographing the setup and using photo imaging software (Photoshop CS6), the actual interfaces of the seal can be determined and the corresponding H can be applied in the model. A corrected pressure $p_{c,c}$ can then be made on the modelled pressure. For each seal, the

highest H value is kept and the lower pressure interface adjusted to the measured interface.

5.2.4 Experimental setup

A basic representation of the setup can be found in figure 5.6. The design [appendix C] consists of a thin channel that has a pressure inlet, a FF inlet and a outlet. Magnets can be placed underneath the channel for creating the necessary seals. Variable parameters to the design are the gap height of the channel (*h*), the foil separating the channel from the magnets (*t*), the number of magnets and the distance between magnets (*d*). To create the channel the setup is made up of two layers of PMMA sandwiching the foil (PE) and a adhesive transfer foil that acts as the adhesive as well as the spacer that creates the height of the gap. The bottom PMMA consists of slits where magnets can be snugly inserted. The PE foil acts as a layer to prevent FF/air leakage.

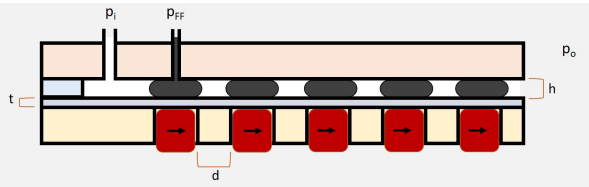

Figure 5.6: A basic representation of the demonstrator showing a cutthrough of the channel with the FF fluid seals. Pressure is increased on the inlet at the left and FF can be added by a seperate inlet. A foil separates the seal from the magnet to secure air thightness of the channel everywhere but at the outlet.

The seals are created by adding FF via the syringe while slightly increasing the pressure in the pressure chamber, thus spreading the FF over all the seals. The intermittent chambers are then pressurized. For the first chamber, this is done by increasing the pressure to the point until the first element start leaking, thus filling the first chamber with air. The next element will start leak through the combined pressure difference of the two element, leaking into the next chamber, and so on. The pressure can be increased until all the elements simultaneously start leaking simultaneously and air escapes from the back end of the whole seal. This pressure is denoted as the the critical pressure p_c of the seal. More FF can be added to possibly increase p_c somewhat. A completed setup with FF seals can be seen in figure 5.7.

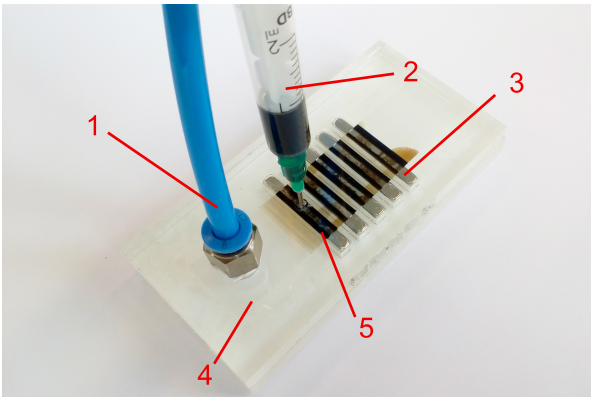

Figure 5.7: The setup, made of laminated PMMA and PE (4), in prepared state. (1) is the air pressure inlet into the inlet chamber. Point (2) is a syringe that works as the FF reservoir and pump. The component denoted at (3) are the magnets and (5) is a FF seal.

To demonstrate the FF transport, a subcritical pressure will be taken and FF injected into the seal. The fluid will fill the first seal and subsequently be transported to the other seals until a new equilibrium has been obtained. Excess FF will build up at the end of the channel.

5.3 Results and discussion

5.3.1 Critical pressure

In the experiment an p_c of 0.50 bar was registered. Taking the picture in figure 5.8, the corrected critical pressures of the 2D and 3D models become, 0.66 bar and 0.46, respectively.

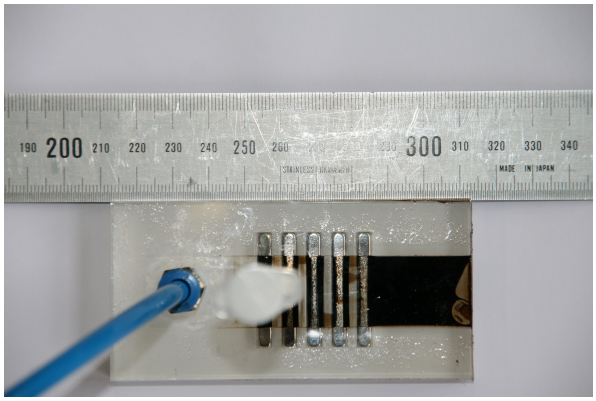

Figure 5.8: Picture of the setup with a measure. Photo imaging software was used to determine the actual location of the seal interfaces.

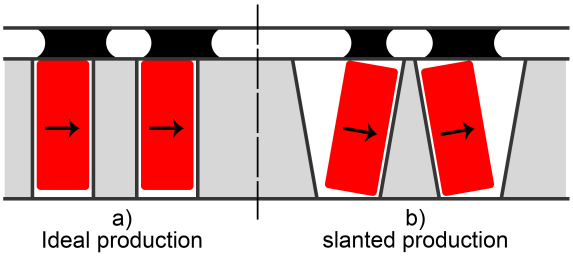

Figure 5.9: In the ideal condition the magnets are oriented parallel in their slots. The slightly diverging beam of the laser has however cut slanted slots. As a result, the magnets line up to the walls beause of the magnetic force between them.

5.3.2 FF transport

The resulting critical pressure from the experiment lays lower than the results of the model and in between the corrected models. This is within the expectation posed for this design. This may result from the fabrication of the set-up: due to the diverging laser beam in the cutting of the PMMA, the magnet slits tend to have slanted edges (figure 5.9). The magnets then align to the walls due to subsequent interaction with the other magnetic fields. This decreases the magnetization in the channel as one edge of the magnet is further away from the channel and, consequently, the pressure drop decreases. The slanting can also alter the distance between magnets somewhat. The properties of the FF can further have a significant influence on the pressure drop. These can possibly deviate from the data sheet. A critical parameter here is the magnetization saturation. It has a linear effect on the pressure drop and can be lower than specified. When looking specifically at the difference between the model and its corrected version, the precision in measuring the interfaces of the elements is somewhat lacking (insufficient resolution of the picture) and misreading of the ruler from the picture due to perspective. This may cause the lower result of the 3D model compared to the experiment.

A sub-critical pressure of 0.40 bar was chosen. When filling the first seal FF is seen added on both sides. After adding a sufficient amount of FF, it starts to be transported to the other seals until a new equilibrium had been obtained. Excess FF has built up at the end of the channel. No leakage of air was detected at the first seal, although if the FF is added too rapidly leaks are detected at the last seal.

The small amount of leakage detected only at the end seal suggest that the air pressure between the seals abruptly increases due to the cascade manner in which the FF is transported from one seal to the next, decreasing the available space between the seals, thus pushing the air out of the pressure chamber. This would also explain why no pressure drop was detected at the first sealing element. With an inlet pressure lower than p_c the pressures in pressure chambers redistribute. The pressure in the first two pressure chambers have decreased while the pressures in the remaining chambers remain unchanged. Figure 5.10 shows the change in chamber pressure with the decrease in inlet chamber pressure. Adding FF will more easily cause a leakage in the last two chambers until the pressure drop over seals restores back to linear.

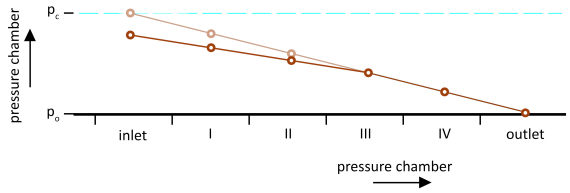

Figure 5.10: Light orange line shows the pressure distribution when seal is at its critical pressure (light orange). Lowering the pressure at the inlet creates a redistribution of the pressures.

5.4 Conclusion

While exploring how to refresh FF in a contactless seal assembly a method has been developed for transporting the fluid passively between sealing elements. This method relies on the attracting force of the next magnet to transport excess FF from the previous sealing element to its own element and then again have it attracted by the next magnet. A model, executed in a 2D and 3D version, was created to be able to predict the maximum critical pressure drop that the setup can hold. The experiments showed that the setup can hold a pressure up to 0.50 bar and doesn't show signs of leakage at the first sealing element situated at the inlet chamber side of the seal assembly. When compared to the models, the results have a reasonable similarity. Due to construction challenges and non-perfect formation of the sealing element the pressure holding capacity is lower than predicted.

The transport mechanism offers promising results where FF can be transported at a subcritical pressure without pressure leak at the first seal. Due to the redistribution of pressures, the detected leaks only affected the last seals.

The result shows that it is possible to replenish FF without losing functionality, which offers a great potential for designing a seal that has an increased lifetime over current seal designs.

Chapter 6

Method for transport of Ferrofluid in a liquid contactless rotational seal

Ferrofluid can effectively be used as a liquid seal for rotary shafts to seal off gasses. The technology tends to be less effective when sealing off liquids, where one major problem is the degradation of FF that comes into contact with the liquid. This paper presents a method for replacing the FF in the seal without pressure loss, in order to improve the lifetime of the seal. A test setup has been designed to comply with all the contemporary knowledge on FF/water interface seals and to improve on it by adding a FF addition method. Using a FEM model to predict the pressure capacity the results show the measured capacity to conform with the model. The setup shows promising results on stability of the seal when water is used as a medium in the pressure chamber

6.1 Introduction

The use of Ferrofluid (FF) in rotational shaft seals is still a novice field when used to seal of liquids. Yet there is an interest from industry to implement this technology for propulsion shafts in ships, as well as many other applications.

The major problem is the failure of the seals in aqueous environment due to degradation [29], which affect the lifetime of these type of seals. When in direct con- tact with water, . In [chapter 5] a mechanism was developed to refresh the FF in the seal, to prevent leaking of the seal over time. The setup however remains stationary and does not take into account the dynamic effects on the seal. Speed differences of the fluids at the seal interface can initiate instability [1], which can lead to mixing of FF with the fluid [10] [32]. Very high rotational speeds can cause centripetal forces [15] to act on the fluid. These phenomena have an adverse effect on the seal lifetime or the pressure drop and are primarily dependent on the peripheral speed of the shaft.

This paper will expand on the mechanism of [chapter 5] of increasing the seal lifetime by removing degraded FF at the water interface through pumping. A new test setup that more closely resembles the real world application where the effects of rotational speed of a shaft will be tested on the FF transport mechanism, will be introduced

6.2 Method

The concept of FF sealing and transport, as well as specific design requirements will be discussed in the following section. This will set the basis for a design which can remove degraded FF to prolong the lifetime of the seal.

6.2.1 FF transport concept

The setup will consist of a rotary shaft with the seal fixed coaxially around it. The setup has a pressure chamber attached to the front end to simulate pressurized fluids at the seal. FF is added at the front end of the assembly (figure 6.1), facilitating the flow of FF to the seals while also diminishing discharge into the pressure chamber. A certain point travel,

the added FF will towards the adjacent magnet that attracts the fluid, thus transporting the FF over the seal assembly. After the last seal the FF can be collected for recycling.

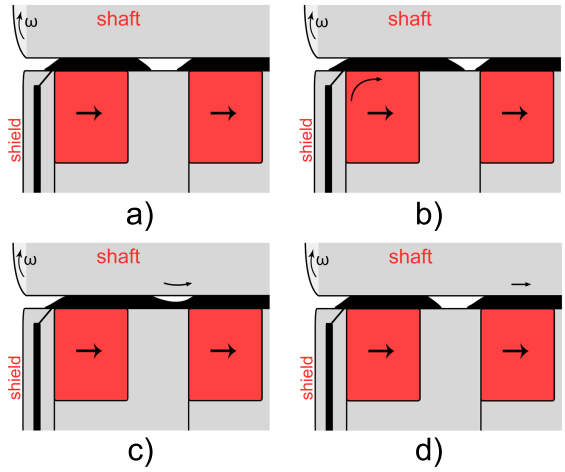

Figure 6.1: Transport of FF. The seal is first a) at equilibruim. Then FF is added b) to the first seal, moving the interface. Magnetic forces c) of the second magnet become more prevalent on the fluid, pulling excess towards it. Finally equilibrium restores d) with the excess fluid now on the second magnet

6.2.2 Sealing concept

The rotation of the shaft will have an influence on the performance of the seal where it can lower the pressure capacity and/or reduce the lifetime of the seal. The pressure capacity is modelled on the static case where the shaft rotational speed is $v = 0m/s$. The gradient of the pressure becomes

$$\nabla p = \mu_0 M_s \nabla H \tag{6.1}$$

where μ_0 is the permeability of air and M_s is the saturation magnetization of the FF. It is important to note is that this equation is only valid for a saturated FF. For a single magnet and a specific FF, equation (6.1) shows that the pressure gradient at a seal is only dependent on the gradient of the magnetic intensity H. Expanding the pressure difference capacity over multiple seals is a summation of the magnets in series. The equation becomes

$$p_i - p_o = \mu_0 M_s (\sum_{i=1}^{n} H_{\mathrm{i},i} - H_{\mathrm{o},i}) \tag{6.2}$$

where H_{i} is the intensity at the higher pressure side of the seal, H_{o} at the lower pressure side, n is the number of sealing rings and i indicate a specific sealing ring. The highest magnet field strength of a magnet is located at the edges. This phenomena can be used to form a seal close to the magnet where a high gradient of H is available.

Interface instability

The shafts rotation has an effect on the behaviour of the fluids at the interface where the fluids meet. When the relative velocity between two fluids at the interface becomes sufficient large, waves form at the interface, and instability occurs. When this instability has fully formed, the fluids start mixing, decreasing the amount of FF in the seal and increasing the contact area at the interface. The point of instability can be predicted by obtaining its criterion using the Rosensweig instability

$$(U_1 - U_2)^2 > \frac{\rho_1 + \rho_2}{\rho_1 \rho_2} \left\{ [2g(\rho_2 - \rho_1)\sigma]^{1/2} + \frac{(\mu_1 - \mu_2)^2}{\mu_1 + \mu_2} (H^2) \right\} \tag{6.3}$$

Where U and ρ are the speed and density of the fluid, respectively, g is the gravity, σ is the surface tension between the two fluids, μ is the permeability of the fluid and H is the magnetic intensity at the interface. The H direction should be parallel to the interface.

The design of the seal should be such that the relative velocity difference between the two fluids is enough to prevent the onset of instability. Peripheral speeds on specifically ships hafts can reach speeds of up to $6m/s$, therefore the design of the seal has to be adapted to mitigate these issues. This can be done by adding a shield to the front end of the seal assembly [10], as is shown in 6.1.

6.2.3 Seal tightness

In the works of Marcin Szczech et al. [16] it is claimed that, when is contact with water, FF seals slowly lose some pressure, coined as *tightness loss*, while the shaft is in motion without failure of the seal. This loss stabilizes over time. Another observation by Szczech is that the critical pressure is dependent on the

speed of the shaft, decreasing with increasing speed with the critical pressure at standstill having the highest value. These phenomena should be reproducible in the setup.

6.2.4 Experimental approach

Setup design

The design of the demonstrator (figure 6.2), named *FFP 02* [appendix D], contains a rotary shaft driven by a motor. The Shaft rotates in a pressure chamber that can hold liquids and pressures.

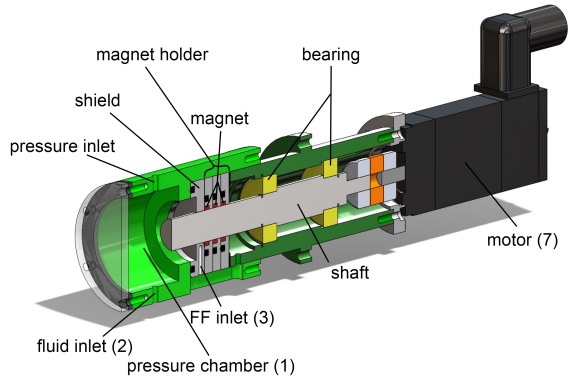

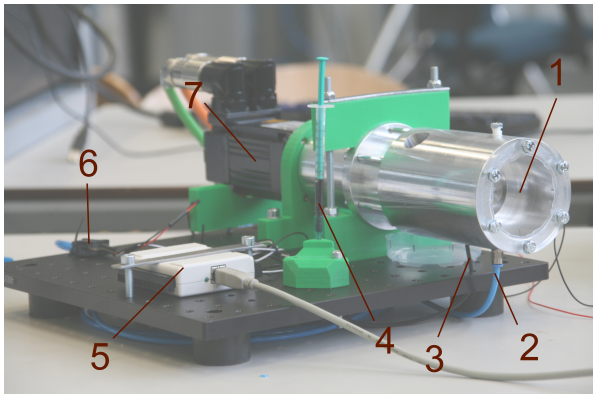

Figure 6.2: Top image is A cutthrough of the *FFP 02*. Colours and tags are used to differentiate between the different components. Numbers correspond with the bottom image. Here, the pressure chamber **(1)** is fed by the inlet **(2)**. The inlet of the FF **(3)** is connected to the syringe **(4)**, used as FF resevoir and pump. A relative pressure sensor **(6)** is connected to a data proccessor **(5)**. The motor **(7)** drives the setup.

A seal assembly, containing the shield and 3 magnetic seals, is placed around the shaft to seal of the chamber. FF can be added at the shield. The pressure chamber can be filled with water and pressurized using compressed air. The seals are created by adding FF via the syringe while slightly increasing the pressure in the pressure chamber, thus spreading the FF over all the seals. The intermittent chambers are then pressurized by increasing the pressure further until all seals start leaking. This pressure is denoted as the the **critical pressure** p_c of the setup. The completed setup with FF seals can be seen in figure 6.2.

Experiments

The experiments will be divided in a static and a dynamic case. In the static case the shaft remains at standstill ($n = 0RPM$). In the the dynamic case, experiments are conducted at speeds between 1000 and $6000RPM$, with increments of 1000.

In the static case the critical pressure $p_{c,s}$ can be determined. This is done by steadily increasing the pressure until air starts leaking through the seal. This failure of the seal can be observed by a sharp decrease in pressure in the chamber, as well as by a bubble sounds coming from at the back end. Another experiment is the testing of the lifetime at standstill, where the chamber is pressurised until $0.95p_{c,s}$ and measured until seal failure.

In the dynamic case, in a first experiment, a **FF transport** test is conducted at a sub critical pressure of $0.5p_{c,s}$. At each incremental velocity step FF is added to the seal in a small burst of $0.1ml$. If the pressure in the chamber decreases with the addition of FF and bubbles can be heard at the back end of the seal, a leak is determined. In a second experiment, the **dynamic critical pressures** $p_{c,d}$ at the different velocity increments is determined. At each speed the pressure is gradually increased until failure of the seal.

Finally the performance of the setup **with water** is tested. An dynamical case experiment is performed where the seal is tested in a water environment at 6000RPM to determine the lifetime of the seal in water. Lastly the FF transport experiment is repeated, now with water in the pressure chamber.

6.2.5 Comsol model

In order to know the magnetization gradient a FEM model is devised. Figure 6.3 is a 2D model that represents a cutthrough figure of the demonstrator. Only half is modelled due to axis symmetry. With the magnetic iso-lines, the figure shows the high gradient near the edges of the magnet and a low point in between the magnets. A total of 3 magnets with thickness $b = 4mm$ are modelled with a flux density of 1.17 Tesla and have the same orientation.

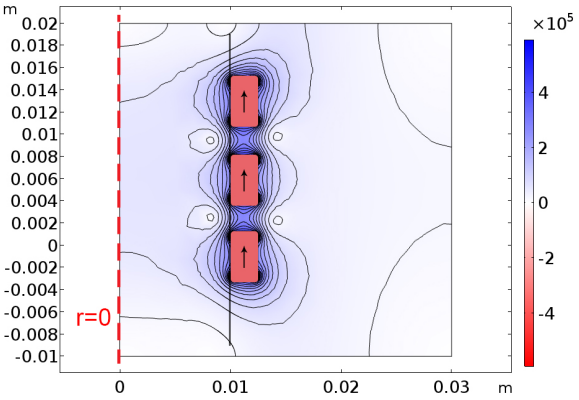

Figure 6.3: Magnetic field lines of the 2D model. Half of the cuttrough has been modelled because of symmetry. Dotted line represents the symmetry line at the center of the shaft. The vertical black line represents the gap of the seal.

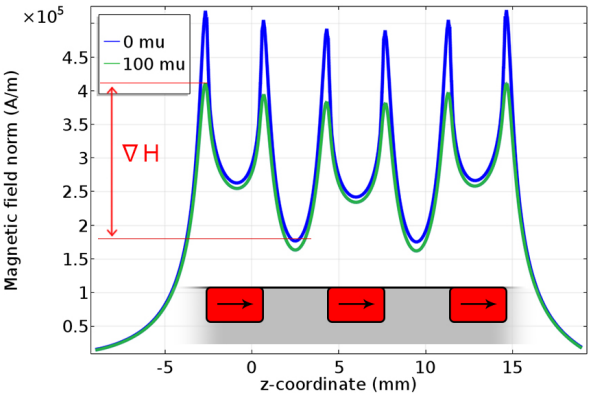

Figure 6.4: Graphs of the magnetic intesity at the top and bottom surfaces in the gap of the seal. Peaks correspond to the edges of the magnets, shown in red. Height is measured from the surface of the magnet.

Table 6.1: Magnetization values from the FEM model for calculating the theoretical maximum pressure

Seal	$H_i * 10^5$ [A/m]	$H_o * 10^5$ [A/m]	Δp [kPa]
1	4.11	1.77	10.30
2	3.84	1.76	9.09
3	4.11	0	18.08

The magnetization field intensity of the model in the gap between magnet and shaft is displayed in figure 6.4. Each spike corresponds to the edge of a magnet and the valley to the furthest distance between two magnet edges. Taking the the fist peak from the green line and its corresponding lowest valley on the blue line forms the H at the two interfaces of the first sealing ring. Repeating this for each seal seal ring gives the values in table 6.1. The assumption is that there is one sealing element per magnet. Two elements will give a slightly higher pressure drop, but is negligible. By implementing the values in equation (6.2), a theoretical maximum pressure of 37.47 kPa can be obtained. The interaction between the sealing rings, resulting from the distance between them, entails in that each ring does not contain the maximum amount FF. This is caused by the attraction forces of the neighbouring rings. The actual p_c thus tends to be lower.

6.3 Results and discussion

6.3.1 Static critical pressure

An average critical pressure of $p_{c,s} = 34.15kPa$ was obtained by increasing the pressure in the chamber until leaking of the seal, which lead to a sharp drop in the graph (figure 6.5). The leaking was accompanied by the sound of air bubbles escaping from the back end of the seal. The difference in critical pressures measured derives from differences in the amount of FF in the seal during the experiments. The small eccentricity in the shaft has also led to different results depending on the rotational orientation of the shaft.

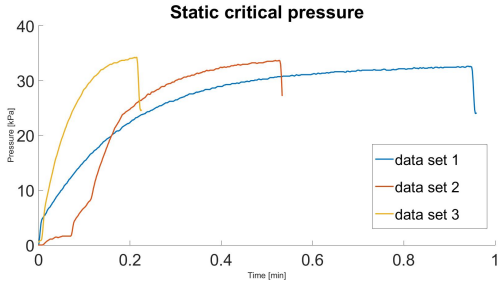

Figure 6.5: An example of three datasets used in calculating the average of $p_{c,s}$. The sharp drop is the result of a leak of the seal. The pressure rise differsbecause of the fact that the presure valve is operated manually.

keeping the setup at a sub-critical pressure of $0.95p_{c,s}$ resulted in leakage after several minutes that continued to leak over several hours. Having the seal at standstill, entices the FF to diffuse slightly towards the magnet, decreasing the pressure drop capacity of a sealing ring. Further more gravity will create a asymmetric sealing ring, weakened at the top due to less FF. This also means that the increased amount at the bottom can lead to undesired FF transport, further decreasing the Pressure drop capacity. If a sealing ring fails, it jettisons FF in the direction of the back end of the seal, which is another form of unwanted FF transport and also has a negative effect on the pressure drop capacity.

6.3.2 Dynamic critical pressure

For the $p_{c,d}$ the values for each speed interval, as well the pressures for $p_{c,s}$ can be found in figure 6.6. The graph shows the pressure drop decreasing with each speed increase. The $p_{c,d}$ for lower speeds was meaured at a higher pressure then the $p_{c,s}$, which was predicted to be the highest pressure. It is suggested that the rotation of the shaft limits the amount of diffusion and asymmetry in the sealing ring, increasing the performance of the seal. This could explain in thehigher sealing capacity. The $p_{c,d}$ gradually dropped over speed. This drop is comparabel to the findings of [16].

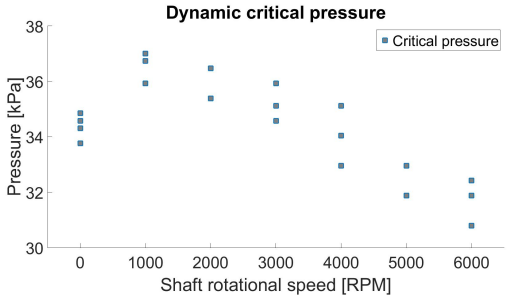

Figure 6.6: At each speed interval a leak test was carried out, resulting in the $p_{c,d}$. The slope indicates the $p_{c,d}$ decreases with speed increase.

6.3.3 FF addition

When adding FF to the seal while the shaft is rotating, no sharp drop in pressure is detected in figure 6.7 for each speed increment. An positive slope for some of the speeds are visible. This has been attributed to the heating of the air by the setup, that is generated by viscous friction of the seal [appendix E]. For experiments at 3000 RMP and 6000 RPM the pressure was reset to 20 kPa. The graph shows that for a FF/air interface the FF transport method works at the given sub critical pressure.

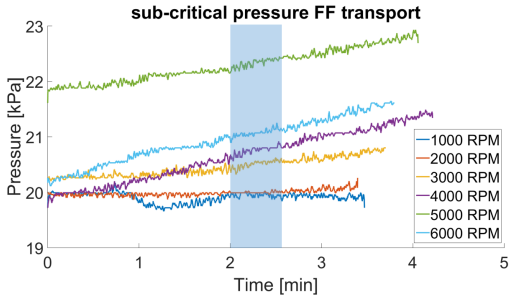

Figure 6.7: Set up is pressurized to $0.5p_{c,s}$ and is run at different speeds where after a certain time (blue area) FF is added to the seal. The rising of the pressure is due to the heating of the setup by viscous friction.

6.3.4 Performance with water

To determine if the design was correctly designed according to the design specifications mentioned in previous chapters a lifetime experiment was conducted. The first test plotted in figure 6.8 is a stepwise increase of the speed at a sub critical pressure. It showed

no sharp pressure decrease although a slight negative slope is visible in accordance with the predictions by [16]. After the maximum speed was attained the test was ended. A full lifetime test was then performed at maximum speed. The graph in figure 6.9 shows the negative slope as before, but later the slope changes in to a positive slope due to the heating of the water. After 51 minutes the seal fails, shown by the sharp pressure decrease in the graph. The seal can hold a sub critical pressure of $22.69kPa$ with an FF/water interface for several minutes, demonstrating that the design behaves comparable to contemporary setups, without further optimisation.

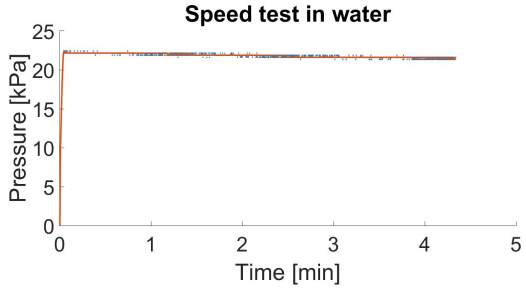

Figure 6.8: starting at $n = 0$ RPM, the speed is increased by increments of 1000 every 30 seconds until 6000 RPM. A slight negative slope is visible

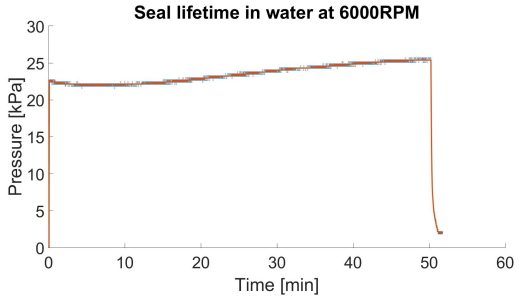

Figure 6.9: At the sub-critical pressure the speed is increased to 6000 RPM. The speed is then maintained until failure of the seal.

Addition of FF with a water interface showed comparable results with respect to the slight negative slope over time. Adding FF at first doesn't lead to failure. However, figure 6.10 shows at 3000 RPM that, while the FF is being added, the pressure sharply decreases and water droplets begin to emerge from the back end of the seal. The relatively quick failure (compared to the lifetime of 51 minutes at max. speed) indicates that the addition of FF was the prime cause for failure. The amount of FF added to the first ring at each interval and the flow rate at which it was administered can have a severe effect. FF that isn't directly taken in the sealing ring and transported further towards the back end acts as excess fluid in front of the seal which can more easily mix with water because it being further away form the magnet. The mixture then can be pressed back into the seal after the addition has stopped, weakening the seal. The location of the FF inlet is also a possible culprit. The inlet resides on the front end of the seal, which could more easily facilitate mixing with the water when FF is administered to the first ring.

Figure 6.10 has also shown that the seal regains a new equilibrium and the leaking stop. The new equilibrium is stable, and it can hold the new pressure, also at higher speeds. The seal is however weakened because now there is water in the chambers. Also some FF has been washed away by the leaked water through the seal. This means small pressure increases lead again to pressure a drop and more droplets forming, further weakening the seal.

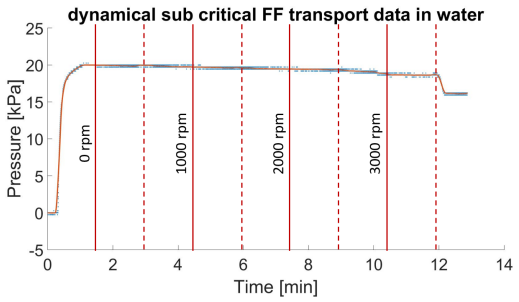

Figure 6.10: Set up is filled with water and pressurized to $0.5p_{c,s}$. At certain moments (solid line) speed is increased, and inbetween (dotted line) FF is added to the seal. At 3000 RPM the seal fails at the moment of FF addition.

A failed seal at standstill was measured to still be able hold a pressure of $15.67kPa$ before failing again. Adding FF to the seal causes the seal to increase its pressure holding capacity to a pressure of $32.42kPa$. This

indicates that a failed seal can be repaired to a certain degree by adding FF to the seal.

6.4 conclusion

A rotation setup was created to observe the effects of FF transport in a liquid seal. The design has been based on the literature under similar conditions to obtain a seal with a high seal life. This includes the of a shield for improved seal stability and also a small gap size to maximize the pressure drop and minimize the interface area. The critical pressure was found to match the analytical model for the static case and in the dynamic case the critical pressure showed to be depended on the rotary speed of the shaft. FF transport was shown to successfully work without seal failure independent on the shaft speed.

The performance of the seal with a water interface showed the capacity to function for 51 minutes with out failure at full speed. The addition of FF however, while the shaft was in motion, has led to the failure of seal prematurely. This suggest that the method for administering the FF has room for improvements and has great possibilities designing a seal with long lifetime.

Chapter 7

Discussion

The following chapter will discuss in a broad sense the results obtained in the experiments mentioned in chapters 5 and 6.

The static case critical pressure is a measure of determining the performance of the seal. The prediction of the critical pressure in the setups shows differences with the measured values. The measured values are lower than the prediction. The suggestion has been made that the design of the seal configurations play an important part in the difference. Aspects like capillary forces, distance between magnets, changes in gap size (excentricity of the shaft) and gravity shape the sealing element and can negatively affect the seal.

Pumping FF to the seal showed in the *FFT 01* the FF being transported from one sealing element to the next. It did not lead to leakage at the first seal. At an inlet pressure lower than p_c the pressures in pressure chambers redistribute, which facilitates the transport. The results show that FF transport can be conducted without failure of the first element.

The FF transport in the *FFP 02* showed that FF can be added to a rotating seal configuration without leakage. No sharp drop in pressure was detected during the addition. Heating of the setup due to viscous friction led to pressure increases. Because the seal was at a sub critical pressure, the seal didn't fail because of surpassing the critical pressure. The results show that for a FF/air interface the FF transport method works at a sub critical pressure.

The seals tend to be sensitive to the flow rate of the FF. If the FF is added too rapidly leaks are detected at the last seal. No pressure drop was detected at the first sealing element because the inlet pressure does not measurably increase due to the FF addition.

Addition of FF with a water interface showed comparable results with respect to the slight negative slope over time. Adding FF at first doesn't lead to failure. At 3000 RPM however, while the FF is being added, the pressure sharply decreases and water droplets begin to emerge from the back end of the seal. The relatively quick failure (compared to the lifetime of 51 minutes at max. speed) indicates that the flow rate of FF pumped was the prime cause for failure. Excess FF in front of the magnet can easily mix with water because of it being further away form the magnet. The location of the FF inlet is also a possible reason. The inlet resides on the front end of the seal, which could more easily facilitate mixing with the water when FF is administered to the first ring.

Chapter 8

Conclusion and recommendation

8.1 Conclusion

This thesis discussed the performance of FF seals for sealing rotary shafts. The thesis had a specific interest in seals designed for sealing other liquids. A problem with a FF/liquid interface is the relative short lifetime of the seal. The goal of this research was to find a mechanical method for (indefinitely) prolonging the lifetime. The following chapter summarizes the most important conclusions of this research.

8.1.1 Literature

- FF seals are liquid, contactless seals with low friction, no stick-slip and are inherently leak free for gasses and vacuums.
- FF seals for sealing liquids have a relative low lifetime in comparison with those sealing pressurized gasses or vacuums.
- Pole pieces are often used in concentrating the magnetic field. The direct use of magnets is also a potent option. Each has their advantages and disadvantages.
- Shields can be used to improve the stability of a seal by decreasing the relative velocity difference between the two fluids at the interface. Shields can also help in reducing the surface of the interface.
- Deterioration is a prime reason for failure in well designed seals.

8.1.2 FF seal design

- The critical pressure of 34.15 kPa closely follows the theoretical value of 37.47 kPa.
- The attracting force of multiple magnets next to each other can be used in transporting excess (deteriorated) FF from the previous sealing element to the next.
- The analytical models are able to predict the theoretical critical pressure.
- Design aspects like distance between sealing elements have an effect on the sealing element and produces a non prefect condition that decreases the sealing capacity.
- Misalignment of the magnets can interfere with the form of the sealing element, negatively affecting the pressure drop
- Physical aspect like gravity, diffusion or capillary forces can (locally) weaken the seal.

8.1.3 FF/water interface performance

- The seal is capable of withstanding a sub critical pressure with a FF/water interface at a speed range between 1000 and 6000 RPM.
- The design of the setup has led to a seal life of 51 minutes which is in line with other setup from literature under comparable conditions.
- In the dynamic case the critical pressure showed to be depended on the rotary speed of the shaft.
- FF transport was shown to successfully work without seal failure independently of the shaft speed.
- The addition of FF has led to the failure of seal prematurely compared to the lifetime of the seal. This suggest that the method for administering the FF has room for improvements

8.2 Recommendation

This thesis has put forward knowledge that can be used in the future to further improve FF seals in an aqueous environment. Most important for this knowledge to prosper is for it to be developed into a working product. For this to happen the most important reccomendation is to research an improved method for pumping FF into the seal and to test this thoroughly with lifetime tests. This can be done on the current design, but should also be tested on other designs as well.

The recommendations have been divided into sections of improvements on three subjects. The first is on improvements that can be done on a research level, finding new areas of application or better understanding the mechanics of FF seals. The second is on improvements on the current design that can profoundly alter the design. The third is on the improvements of the setup itself that can be done without much redesigning.

8.2.1 Research improvements

- Create a better understanding for the slight decrease in pressure for a FF/water interface when the shaft is in motion
- improving the understanding of the dynamic case critical pressure and why this is dependent on the speed.
- Research the influence of temperature on the performance of the FF seal
- Research on improving FF's implemented in FF/water interface seals
- finding out what the effect of cyclical pressure loads have on seal with a FF/water interface
- What are the effects of gravity and diffusion on the FF seal when scaling up large size shaft (in the order of $1m$)

8.2.2 Design improvements

- Replace the Aluminium 7075 with an other aluminium or non magnetic metal. This specific aluminium is not very corrosion resilient when in direct contact with water.
- Increase the size of the pressure chamber to possibly diminish the effect of turbulence the water can have on the seal.

- Optimize the geometry of the shield and/ the magnet holders.
- Change the geometry and/or location of the FF inlet. Examples are having the inlet before/after/above the first sealing element or multiple inlet locations
- Add cooling to the setup to better control the temperature of the setup

8.2.3 Setup improvements

- Replace the PMMA plastic pressure cover with more resilient and safe plastic (PMMA splinters when it fails)
- Add control to the setup to more consistently perform experiment. Examples are remote control of the motor, autonomously performing preprogrammed reference speeds and sensing seal failure resulting in stopping the motor and measurements
- Using a throttling valve in combination with a ball valve to produce a more consistent pressure increase in the pressure chamber when preforming critical pressure tests
- use a beter method for pumping FF to the seal to control the flow rate of FF
- Add a rubber ring between the bearing housing part and the back end magnet holder to prevent excess FF from creeping into unwanted places.
- Use a check valve to compensate for pressure increase due to heating of the setup

Appendix A

Generation 1 Ferrofluid shaft seal set-up

In this appendix the details of the *FFP 01* set-up are addressed. An explanation of the functionality will be given, followed by detailed descriptions and blueprints of the various parts.

A.1 Functionality

The *FFP 01* was built with the intention to better understand the principles of FF sealing as well as the practical issues that can arise with building such a set-up. Issues like material selection, fabrication limitations and effects due to an aqueous environment are important to understand for further improvement of the set-up for possible later generation demonstrators. The set-up, as seen in figure A.1, constist of a hull with a hole in it, through which a shaft runs. This shaft can freely rotate, with one side on the dry "inside of the ship", and the other in a water container, or the "outside of the ship". A mounting spot serves as a way to easily interchange seal modules for experiments and the shaft diameters can just as easily be altered. The *FFP 01* was designed to create an intuitive demonstrater where the viewer can see all the components and play with them.

With the *FFP 01* it's possible to recreate experiments from literature an validate the results. The flexible design grants the possibility to experiment with gap size, pole piece geometry, magnet configuration, number of seals and, with some adjustments to the design, pressure. At the same time the set-up lends the opportunity to mount novel sealing concepts for prototype testing.

A.1.1 Hull

To simulate the hull of a ship or, in general, the part of the system that is in contact with the environment that is to be excluded a thick piece of aluminium is used. It has a hole through which the shaft extends into the environment. The hole diameter is wider than the shaft by a few millimetres to facilitate fluids that have leaked past the seal to flow through to the sensor. the hull contains two tapped holes and a centering ring to mount and center the sealing module to the hull. Figure A.3 contains the blueprint for this part.

A.1.2 Shaft

The Shaft rotates on two bearings and can be actuated by a motor via a belt drive or direct actuation and the end of the shaft. The front end has a narrow part and tapped hole for mounting the cylinder. The narrowing is used to allow for a larger range of diameter variation. The shaft is made from 403 stainless steel. This is first off due to the yield strength the material

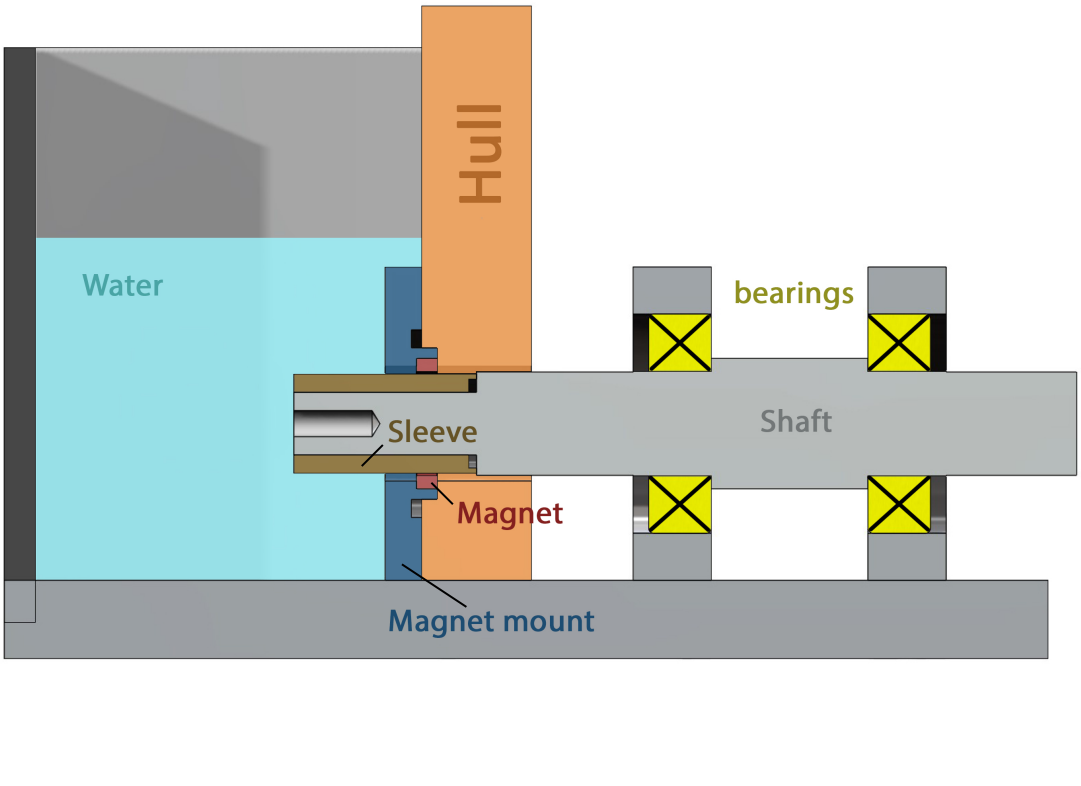

Figure A.1: a cutthrough of the FFP 01. Colours are used to differentiate between the different components.

can withstand, as well as barely corroding in a aqueous environment. Secondly, the material has a very low magnetic permeability so it will have little effect on the magnetic field lines of the seal. Figure A.8 contains the blueprint for this part.

A.1.3 Shaft cylinder

To be able to vary the diameter of the a cylinder was devised that can slip over the shaft and fastened. With this it's possible to make several cylinders with different diameters or materials. As a default brass is used because of its low corrosiveness in water and with the stainless steel shaft, as well as its low magnetic permeability. The cylinder has a groove for placing a rubber o-ring. Figure A.7 contains the blueprint for this part.

A.1.4 Ball bearing

For the Demonstrator two **E2.6004-2Z/C3 from SKF** have been used because of the low friction.

A.1.5 Seal module

The Seal module is the assembly of parts that make up the seal configuration. Having the modular concept makes it possible to attach different kind of configurations to the hull. A groove and rubber o-ring create a water tight seal so no can fluid leak through other than at the testing seal. A centring ring on the module ensures that its can be accurately coaxially mounted. The default module is a single magnet with no pole pieces. Figure A.6 contains the blueprint of a single magnet holder.

A.1.6 Magnet

The magnet used as default for this set-up is the **R25x20x04Ni-N35** from HKCM

A.1.7 Water container

For recreating the environment a container of $3mm$ PMMA clear plastic was used and glued into place using silicon kit. The container makes it possible to fully submerged the sealing module. The container could be altered to also hold higher pressures.

A.1.8 Sensor

The Sensor is placed at the hole of the hull, under the shaft to sense when the system starts leaking. It is glued in to place using silicon kit and is connected to the Arduino system.

A.1.9 miscellaneous

To bolt the seal module and shaft cylinder to the set-up Stainless steel bolts and washers were used. Standard rubber o-ring were used for creating a water tight seal at interface of the above mentioned parts and the set-up. To glue the PMMA parts of the water container «» silicon kit for aquarium.

A.2 Design

The following figures contain the blueprints of the FFP 01. Figure A.2 the set-up as a whole, whereas the other figures contain the individual components of the set-up.

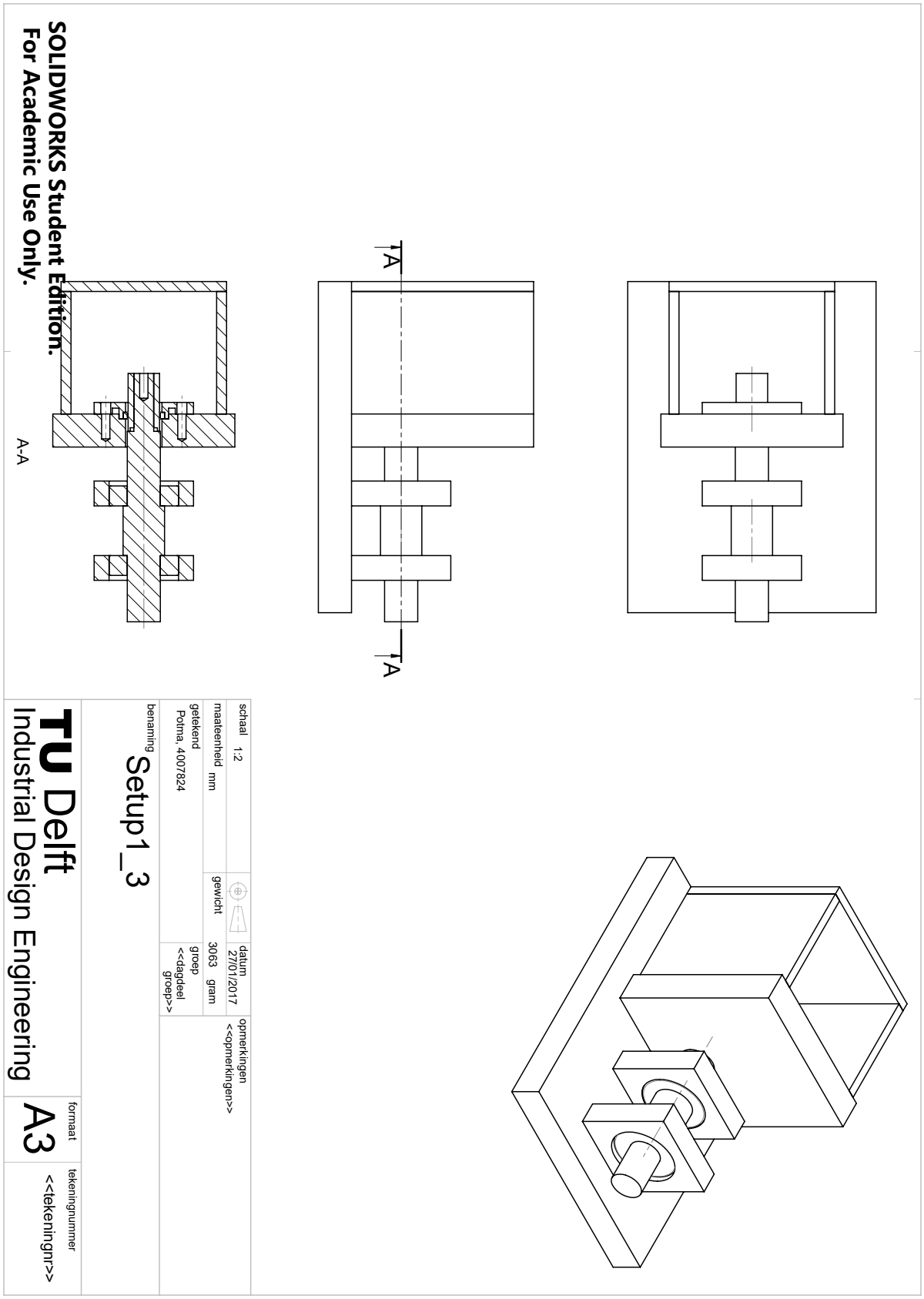

Figure A.2: Multiple views and a cu through of the setup

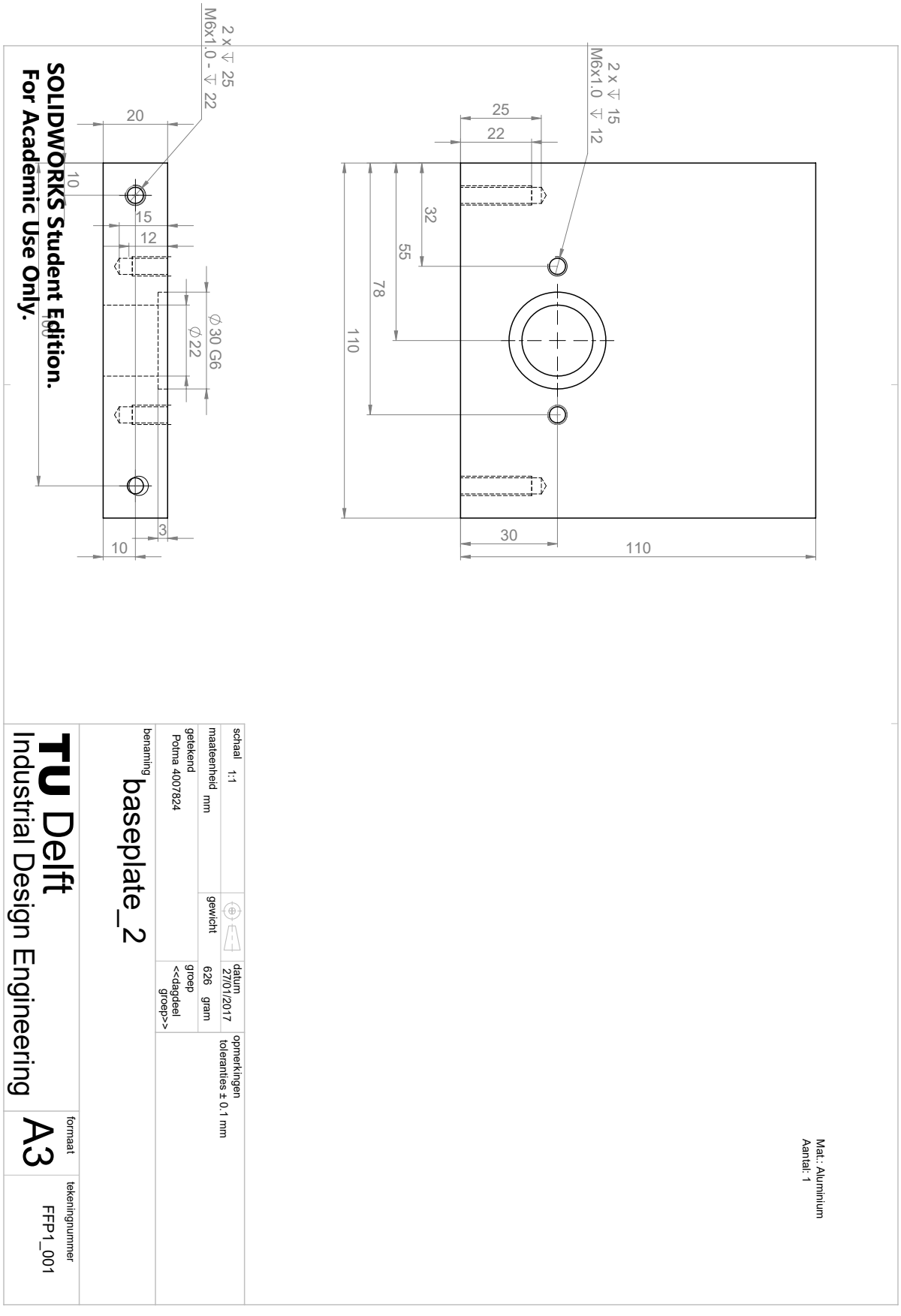

Figure A.3: Blueprint of the baseplate

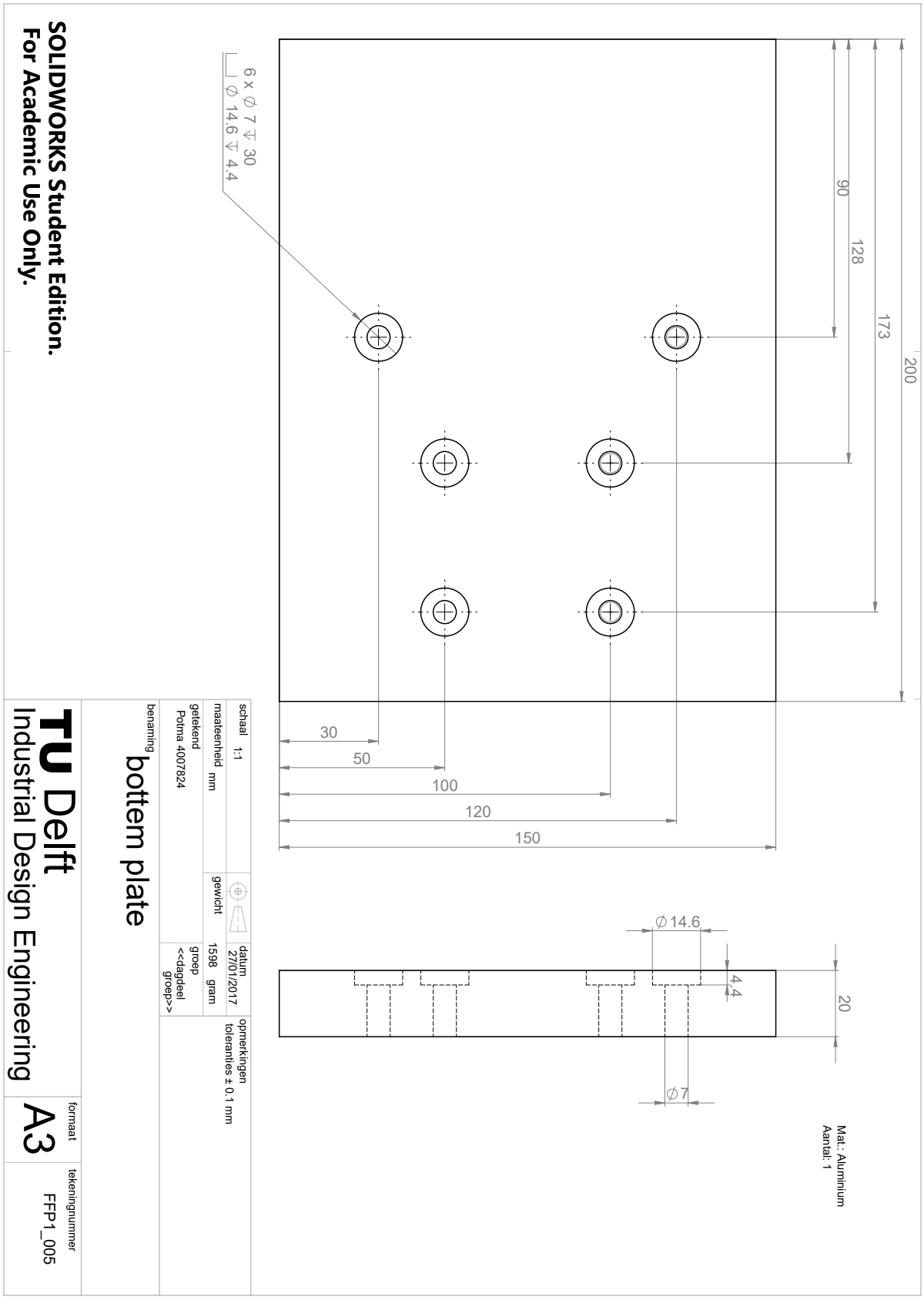

Figure A.4: Blueprint of the bottomplate

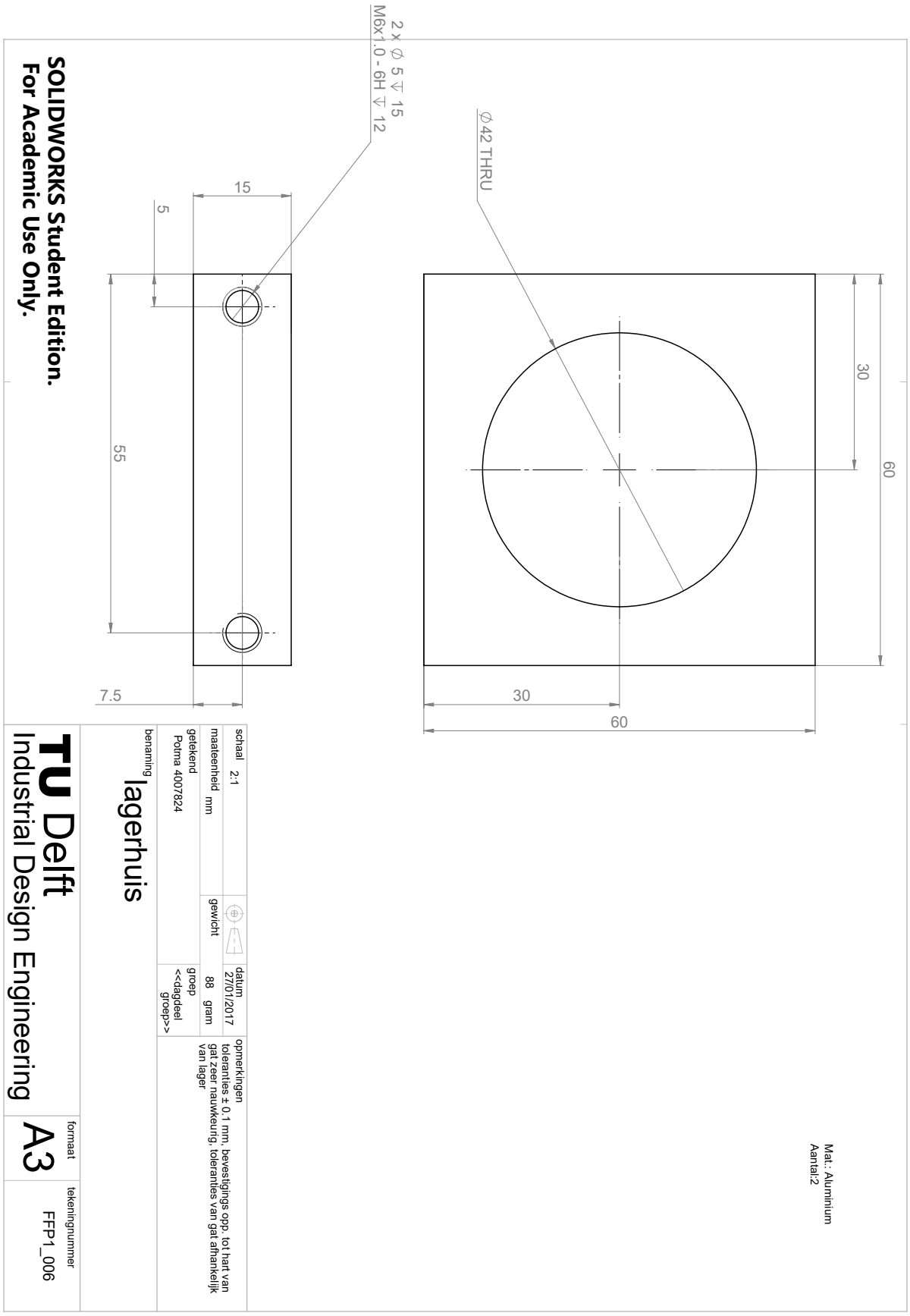

Figure A.5: Blueprint of the bearing housing

Figure A.6: Blueprint of the magnet housing

Figure A.7: Blueprint of the shaft tube

Figure A.8: Blueprint of the shaft

Appendix B

Control

To operate the *FFP 01* a control sytem has been devised to facilitate actuating the shaft, read out sensors and process data. For this the choice was made to use a Arduino module. The Arduino can be controlled using software written by the user. This enables the possibility to control the set-up from a PC connection, as well as functioning autonomously on a power supply. In the following sections The schematic design of the control system is discussed, as well as the hardware used and software written for this set-up.

B.1 Design

The functionality of the design can be divided into three segments; the *Water detection sensor*, which can send an analogue signal to the Arduino in the event the sensor being tripped, the *Motor control*, which has speed control and can be turned on and of by user or the Arduino input, and the Arduino, which is responsible for the software and communication between the pc and the other segments.

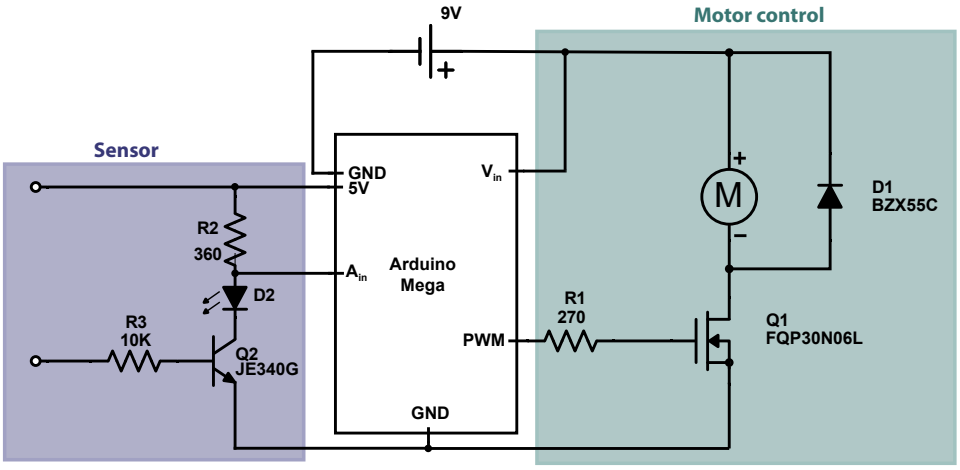

Figure B.1: Schematic of the Control system. Highlighted are the different subparts of the design.

B.1.1 Water detection sensor

The sensor uses a 5V power source from the Arduino. The sensor has two conducting wire in an open-end configuration as show in the figure. This part functions as the 'sensing' part

of the sensor. In the open-end situation, the transistor is closed and the voltage at A_{in} is maximum (5V). The sensor trips when the conducting wires short-circuit. This happens when a conducting material connects the two wires, in this case water. When this happens, the transistor opens and the voltage at A_{in} drops. To add a visual recognition to the sensor being tripped a LED is added in the schematic. It turns on the moment the transistor opens.

B.1.2 Motor control

The motor control directly uses the 9V volt supply. The Pulse Width Modulation (PWM) is used to create a specific voltage drop over the motor by turning the transistor on and off rapidly. With this it's possible to control the speed of the motor. setting the PWM to zero turns the motor off. A diode is connected parallel to the motor to prevent negative voltage spikes from damaging the transistor or Arduino. These spikes arise when the power to the motor is turned off.

B.1.3 Arduino

The Arduino is powered by the 9V supply via the V_{in} and the ground (GND). It's connected to the PC using a USB cable. Using the software the Arduino can control the motor and read out the sensor. With its internal memory data can be stored for when its not connected to the PC and is running a test.

B.2 Hardware

In the following table are the specifications for the different components of the control system

Table B.1: A list of hardware used in the set-up

Arduino	Mega 2560 R3
Q1	FQP30N06L N-channel MOSFET
Q2	JE340G NPN Silicon Transistor
M	Como Drills DC Motor, 7.98 W, 6 $\longrightarrow$ 15 V dc, 78.4 gcm, 9869 rpm, 2.305mm Shaft Diameter
D1	BZX55C (12V)
D2	basic LED

B.3 Software

B.3.1 functions

The software has been written object oriënted using function callback. Default to the Arduino coding is a *setup* funciton, called when the script is started up, that initializes the program, and the *loop* function, which loops during the program is active. The function that have been used in this script are

- **setup()**: makes a connection between the PC and the Arduino and executes *Startup-Menue()*.
- **loop()**: Contains all calls for functions based on the chosen menu item.
- **timer()**: Precise timer with millisecond accuracy and doesn't suffer from roll-over.
- **StopTimer()**: Stops the tickEvent from the loop function
- **ResetTimer()**: Sets all timer parameters back to zero.

- **SaveTime()**: Savs the timer parameters to an object and szves that object to th Arduino's internal memory using the EEPROM.h file.
- **doIncreaseSpeed()**: increases the speed of the motor incrementally. If the sensor is not tripped at full speed the motor is turned off using *StopSpeedTest()*.
- **StopSpeedTest()**: Stops the function t.every() from Timer.h in *loop* that calls *doIncreaseSpeed()*.
- **doPrintSensorReadings()**: Prints the sensor value as well as the output value.
- **StopSensorReadings()**: Stops the function t.every() from Timer.h in *loop* that calls *doPrintSensorReadings()*.
- **StartupMenue()**: prints a list of items. By entering the corresponding number a test can be started.

B.3.2 Code

The following box contains the source code for the Arduino.

```
#include <EEPROM.h>
#include "Timer.h"
Timer t;

// constants
  const int analogInPin = A3;  // Analog input pin that the potentiometer is
    attached to
  const int analogOutPin = 9; // Analog output pin that the LED is attached to
  const int interval = 1000;
  byte seconds ;
  byte minutes ;
  byte hours ;
  byte days;
  int tickEvent;
  int CritSpeedEvent;
  int SensorReadingEvent;
  int eeAddress = 0;
  int ActiveTest;
  int DeActivate = 0;
  int Activate = 1;

// variables
  int motorPin = 3;
  int speed_high = 200;
  int speed_low = 0;
  int sensorValue = 0;        // value read from the pot
  int outputValue = 0;        // value output to the PWM (analog out)
  int procedure = 0;           // activate begin op 0 om de motor uit te hebben
  unsigned long previousTime;
  int fStop;
  int fSave;
  int aRetrievedTime; //Variable to retrieve from EEPROM.
  int aSpeed;

struct MyObject{
  byte oDay;
  byte oHour;
  byte oMinute;
  byte oSeconde;;
};

//+-+-+-+-+-+-+-+-+-+-+-+-+-+-+-+-+-+-+-+-+-+-+-+-+-+-+-+-+-+-+-+-+-+-+-+-+-+-+
void setup()
{
  pinMode(motorPin, OUTPUT);
```

```
  Serial.begin(9600);
  while (! Serial);
  StartupMenue();
//  analogWrite(motorPin, speed_high);

}


//+-+-+-+-+-+-+-+-+-+-+-+-+-+-+-+-+-+-+-+-+-+-+-+-+-+-+-+-+-+-+-+-+-+-+-+-+-+-+-+-+
void loop()
{
  //check for a command from the searial
  if (Serial.available())
  {
    procedure = Serial.parseInt();

    // turn of motor and tests
    if (procedure == 0)
    {
      analogWrite(motorPin, speed_low);
      StopTimer();
      ResetTimer();
      StopSensorReadings();
      StopSpeedTest();
      ActiveTest = DeActivate;
      Serial.println("");
      Serial.println("Test stopped");
      Serial.println("");

      StartupMenue();
    }

    // long run test actvation
    else if (procedure == 1)
    {
        previousTime = 0; //zet de timer op nul
        Serial.println("Starting enduance test");
        analogWrite(motorPin, speed_high);
        tickEvent = t.every(1000, timer);


        ActiveTest = Activate;
    }


    // return saved data
    else if (procedure == 2 )
    {
      MyObject aRetrievedTime; //Variable to store custom object read from EEPROM.
      EEPROM.get(eeAddress, aRetrievedTime);
      String aRetrievedTimeString = String(aRetrievedTime.oDay) + " days,  " +
    String(aRetrievedTime.oHour) + ":" + String(aRetrievedTime.oMinute) + ":" +
    String(aRetrievedTime.oSeconde);

      Serial.println(aRetrievedTimeString);
//        ActiveTest = Activate;
//        activate = DeActivate; //slordige manier om de print maar een keer te laten
     gebeuren
    }

    // lees sensor uit op de serial monitor
    else if (procedure == 3)
    {
```

```
      Serial.println ("starting sensor test");
      ActiveTest = DeActivate;
      SensorReadingEvent = t.every(500, doPrintSensorReadings);
    }

    //critical speed test
    else if (procedure == 4)
    {
//      analogWrite(motorPin, speed_low);
//      StopTimer();
      Serial.println ("starting critical speed test");
      previousTime = 0; //zet de timer op nul
      aSpeed = 0;
      tickEvent = t.every(1000, timer);
      CritSpeedEvent = t.every(5000, doIncreaseSpeed);
      ActiveTest = Activate;
//      activate = DeActivate; //slordige manier om de print maar een keer te laten gebeuren
    }
    // timer test
    else if (procedure == 5)
    {
      previousTime = 0; //zet de timer op nul
      tickEvent = t.every(1000, timer);
    }

    else if (procedure > 5 || procedure < -1)
    {
      Serial.println("incorrect value entered") ;
    }
  } // end serial.available


  // read the analog in value:
  sensorValue = analogRead(analogInPin);
  // map it to the range of the analog out:
  outputValue = map(sensorValue, 0, 1023, 255, 0);
  // change the analog out value:
//  analogWrite(analogOutPin, outputValue);

  if  (outputValue > 120 && ActiveTest != DeActivate)
  {
    analogWrite(motorPin, speed_low);
    Serial.println("sensor triggered, test ended");

    StopTimer();
    SaveTime();
    ResetTimer();
//    t.stop(SensorReadingEvent);
    StopSpeedTest();
   ActiveTest = DeActivate;
    Serial.println("Time saved");
  }

  t.update();


}

//+-+-+-+-+-+-+-+-+-+-+-+-+-+-+-+-+-+-+-+-+-+-+-+-+-+-+-+-+-+-+-+-+-+-+-+-+-+-+-+
void timer()
{
  unsigned long currentTime = millis();
```

```
//   if (millis() >= (previousTime))
//   {
      previousTime = previousTime + 1000;  // use 1000000 for uS
      seconds = seconds +1;
      if (seconds == 60)
      {
         seconds = 0;
         minutes = minutes +1;
         previousTime = 0;
      }
      if (minutes == 60)
      {
         minutes = 0;
         hours = hours +1;
      }
      if (hours == 24)
      {
         hours = 0;
         days = days + 1;
      }
  Serial.print (days, DEC);
  Serial.print (" days,  ");
  Serial.print (hours, DEC);
  Serial.print (":");
  Serial.print (minutes,DEC);
  Serial.print (":");
  Serial.println(seconds,DEC);
//   Serial.print("current = ");
//   Serial.print(currentTime);
//   Serial.print("\t previous = ");
//   Serial.println(previousTime);
//   } // end 1 second

//   delay(1000); //This will ensure one loop per second

} // end loop

//+-+-+-+-+-+-+-+-+-+-+-+-+-+-+-+-+-+-+-+-+-+-+-+-+-+-+-+-+-+-+-+-+-+-+-+-+-+-+-+-+
void StopTimer()
{
  t.stop(tickEvent);
}


//+-+-+-+-+-+-+-+-+-+-+-+-+-+-+-+-+-+-+-+-+-+-+-+-+-+-+-+-+-+-+-+-+-+-+-+-+-+-+-+-+
void ResetTimer()
{
  seconds = 0;
  minutes = 0;
  hours   = 0;
  days    = 0;
}
//+-+-+-+-+-+-+-+-+-+-+-+-+-+-+-+-+-+-+-+-+-+-+-+-+-+-+-+-+-+-+-+-+-+-+-+-+-+-+-+-+
void SaveTime()
{
  MyObject customVar = {
    days,
    hours,
    minutes,
    seconds
  };

   EEPROM.put(eeAddress, customVar);
```

```
}

//+-+-+-+-+-+-+-+-+-+-+-+-+-+-+-+-+-+-+-+-+-+-+-+-+-+-+-+-+-+-+-+-+-+-+-+-+-+-+-+-+
void doIncreaseSpeed()
{
  if (aSpeed == 255)
  {
    StopSpeedTest();
    Serial.println ("maximum speed attained. sensor did not trip");
  }
  else
  {
    aSpeed = aSpeed + 5;
    analogWrite(motorPin, aSpeed);
    Serial.println ("current speed is : " + String(aSpeed));
  }
}

//+-+-+-+-+-+-+-+-+-+-+-+-+-+-+-+-+-+-+-+-+-+-+-+-+-+-+-+-+-+-+-+-+-+-+-+-+-+-+-+-+
void StopSpeedTest()
{
  t.stop(CritSpeedEvent);
}

//+-+-+-+-+-+-+-+-+-+-+-+-+-+-+-+-+-+-+-+-+-+-+-+-+-+-+-+-+-+-+-+-+-+-+-+-+-+-+-+-+
void doPrintSensorReadings()
{
  // print the results to the serial monitor:
  Serial.print("sensor = ");
  Serial.print(sensorValue);
  Serial.print("\t output = ");
  Serial.println(outputValue);
}

//+-+-+-+-+-+-+-+-+-+-+-+-+-+-+-+-+-+-+-+-+-+-+-+-+-+-+-+-+-+-+-+-+-+-+-+-+-+-+-+-+
void StopSensorReadings()
{
  t.stop(SensorReadingEvent);
}

//+-+-+-+-+-+-+-+-+-+-+-+-+-+-+-+-+-+-+-+-+-+-+-+-+-+-+-+-+-+-+-+-+-+-+-+-+-+-+-+-+
void StartupMenue()
{
  Serial.println("Start menue. type:");
  Serial.println("'1' to do a endurance test");
  Serial.println("'2' to retrieve saved data");
  Serial.println("'3' to do a sensor test");
  Serial.println("'4' to do a critical speed test");
  Serial.println("'5' to do a timer test, and");
  Serial.println("'0' to stop testing");
  Serial.println("");
}
```

FFP_03.ino

Appendix C

Ferrofluid transport set-up

In this appendix the details of the *FFT 01* set-up are adressed. An explanation of of the functionality will be given followed by detailed descriptions and blueprints of the various parts.

C.1 Functionality

FFT 01 was build to demonstrate the capability of transporting FF from one magnet to the next using only the external pressure and the addition of fresh FF. To demonstrate this function a simplified 2D design was created without moving parts. The design consists of a small channel that resembles the gap of a FF seal that can be pressurized on one side to simulate the external water pressure. Over the lenght of the channel magets are placed to create FF seals.

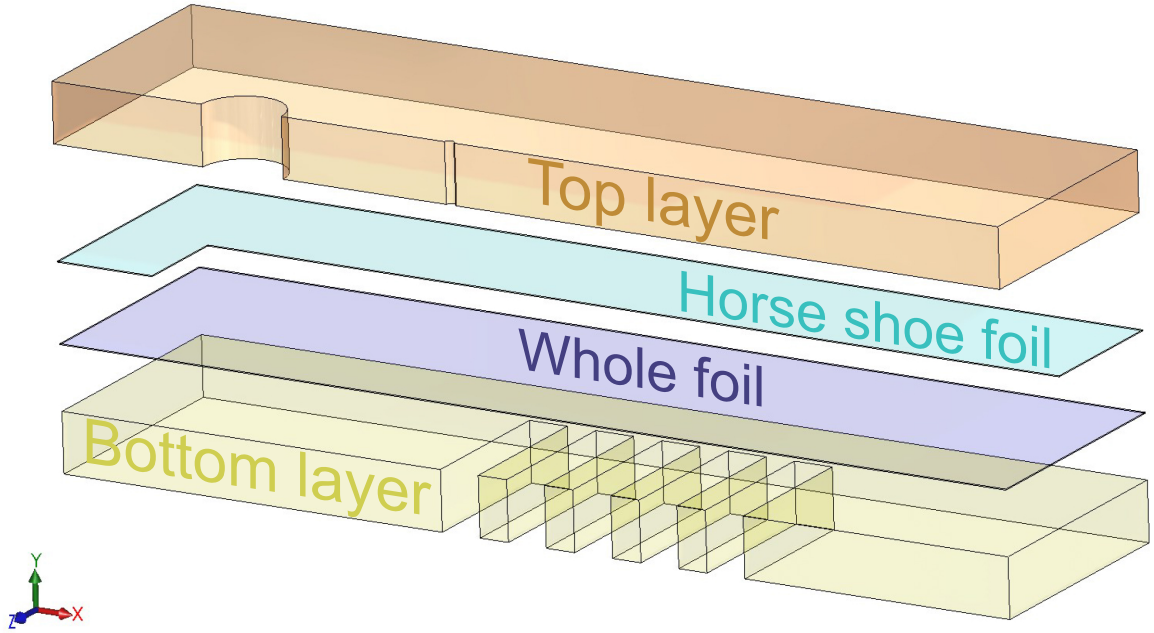

Figure C.1: An exploded cutthrough of the FFT 01. Colours are used to differentiate between the different components.

The Demonstrator is created by laminating several layers of plastic using transfer foil. Figure C.1 shows a exploded cut through of the demonstrator. The following subsections highlight the parts.

C.1.1 Top layer

The top layer is a 6 mm PMMA clear plastic sheet with an hole for mounting the pressure coupling and a hole for mounting the syringe coupling.

C.1.2 Horseshoe foil

The horseshoe foil determines the shape and the gap size of the channel. It has transfer foil on both sides in the same shape to glue it to the top layer and the whole foil. In earlier versions clear PE foils with thickness ranging from 300 down to 100 μm were used to set the gap size, with the transfer foil thickness adding to the gap size. In the most recent version the foil was left out and only a single layer of transfer foil was used in the shape of the horseshoe to simultaneously act as the channel shape, gap size and as the adhesive between the top layer and the whole foil.

C.1.3 Whole foil

This layer functions as a way to make the channel air-tight. As the magnets will not perfectly fill the compartments in the bottom layer fluids can seep past this point, which is unwanted. The foil, made from 100 μm clear PE, prevents this by being glued to the horseshoe foil (or in the most recent one, directly to the top layer). Transfer foil is also used to adhere the foil to the bottom layer. The adhesion foil is cut away at the magnet to decrease the distance between the magnet surface and the lower interface of the channel.

C.1.4 Bottom layer

The bottom layer is a 6 mm PMMA clear plastic sheet which has compartments where magnets can be snugly fit in.

C.1.5 Transfer foil

The transfer foil is a clear adhesive used to laminate the demonstrator. It is **3M Tapesheet 7955 MP (or 468MP)** with a thickness of 127 μm.

C.1.6 Magnets

The magnets used in this demonstrator are five **Magnet-Cuboid Q32x08x04Ni-38H** from **HKCM**.

C.2 Design

The following figures contain the blueprints of the FFT 01. The figures contain the blueprints of the individual components of the demonstrator.

Figure C.2: Blueprint of the bottom part

Figure C.3: Blueprint of the top part

Figure C.4: Blueprint of the horseshoe foil

Figure C.5: Blueprint of the whole foil

Appendix D

Generation 2 Ferrofluid shaft seal set-up

D.1 Functionality

The second generation of the setup, or *FFP 02*, is a demonstrator to show the workings principle of FF transport between seals in an actual working shaft assembly. The setup, as seen in the cut through figure D.1, consist of a shaft powered by an electro motor passing through a "ships hull" into a water reservoir. The reservoir can be pressurized to simulate different depth pressures. A seal assembly can be placed around the shaft, of which the configuration can be altered. This is in respect to the amount of seals, inter seal distance and the use of shields. Similar to the *FFT 01*, the setup possesses a supply mechanism for the application of fresh FF to the first seal. excess FF can be collected a the rear of the seal assembly.

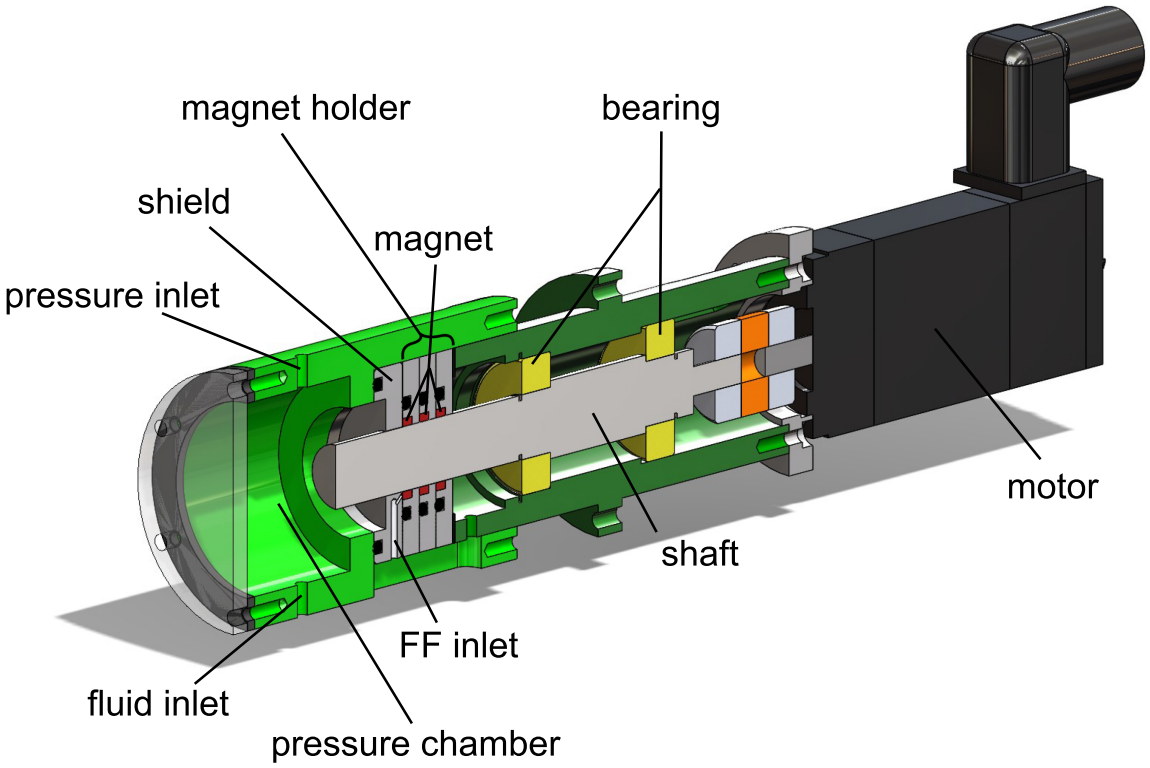

Figure D.1: A cutthrough of the FFP 02. Colours and tags are used to differentiate between the different components.

D.1.1 Seal housing

This part is intended to hold the seal assembly and the reservoir. The parts of the assembly can slide in from the right side, and o-rings assure pressure can only seep past the FF interface part of the seal. The reservoir cover can be bolted to the left side of the part and there are two inlets for filling or purging the reservoir. On the bottom is a slit where the FF supply mechanism can be coupled to the seal and a purge for excess FF at the rear. The right side also has tapered holes to fix the shaft assembly to it.

D.1.2 Shaft Housing

The Shaft housing holds all the moving parts. In it the shaft with accompanying ball bearings are installed. an outer ring with holes is used to mount the part to the Seal housing. On the right side the motor can be connected to the housing, with a flexible coupling connecting the motor shaft to the setup shaft.

D.1.3 Shaft

The shaft has been fabricated from 304 Stainless steel which, like for *FFP 01*, has a very high yield strength, has little corrosion in an aqueous environment and has a very low magnetizability. Its dimensions on the left side have very low tolerance to accommodate for the small gap size necessary for this setup.

D.1.4 Magnet holder

The magnet holder is a very simple disc in which a magnet can be nestled, as well as an o-ring. The thickness of the ring can be altered to change the distance between the seals.

D.1.5 Shield

The shield is used to increase the maximum rotation speed the FF seals can hold before failure. It also doubles as a directed supply nozzle for the fresh FF. It also has a o-ring nestled in it. The shape and size of the seal can be changed to optimize its performance.

D.1.6 Reservoir cover

The cover is a 6 mm PMMA clear plastic sheet cut with the use of laser cutting.

D.1.7 Motor

The motor is a **CMP40S Synchronous motor** from **SEW**. It was chosen for the high precision in rotation speed control, permissible maximum rotational speed and torque delivered at the required rotational speed. The motor comes with an encoder, controller and cables. the coupling used is a **KTR Jaw Coupling ROTEX14** from **RS**.

D.1.8 bearings

For the Demonstrator two **E2.6004-2Z/C3** from **SKF** have been used because of the low friction.

D.1.9 magnets

The magnet used as default for this set-up is the **R25x20x04Ni-N35** from **HKCM**.

D.2 Design

The following figures contain the blueprints of the FFP 02. The figures contain the individual components of the set-up.

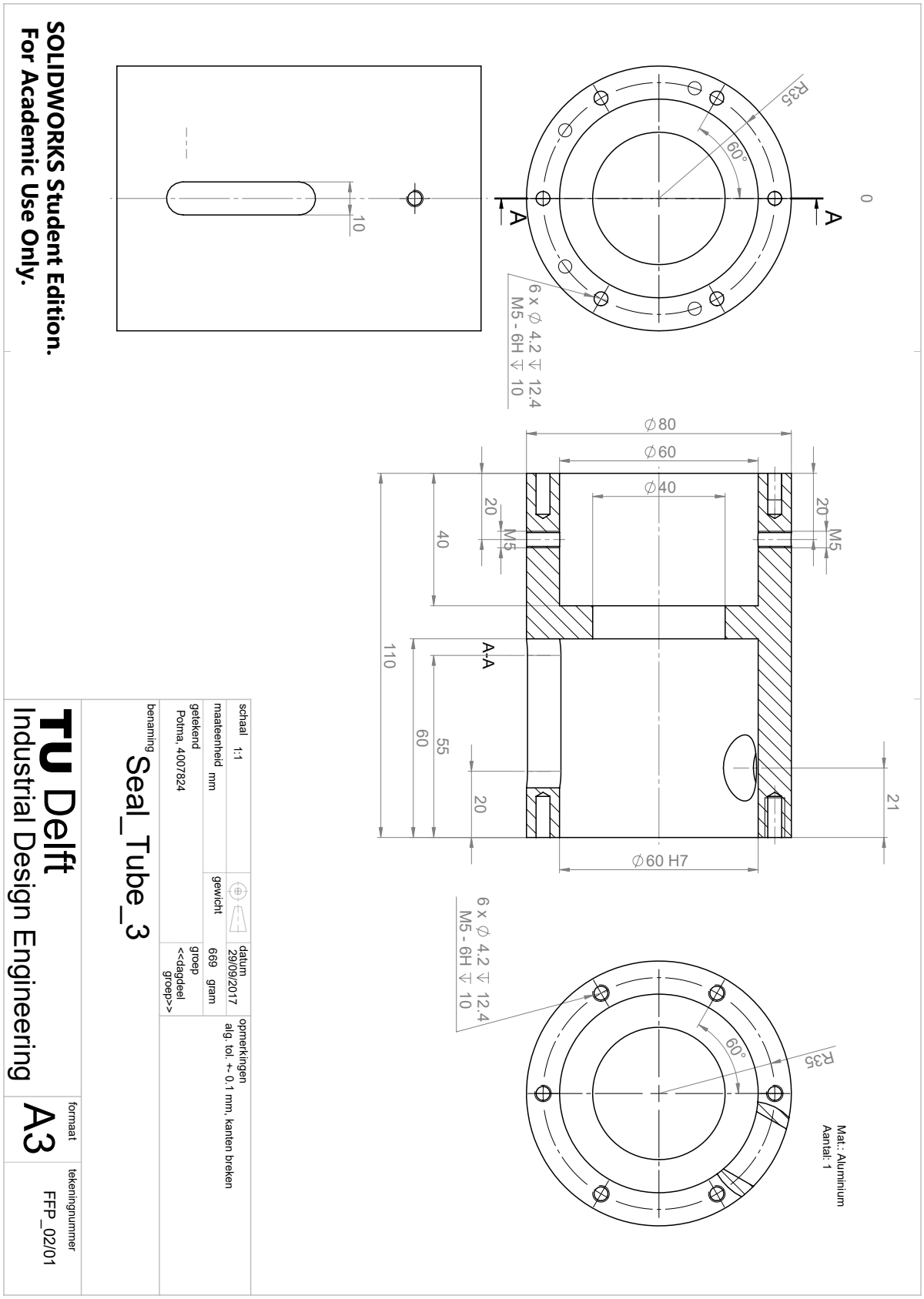

Figure D.2: Blueprint of the seal housing

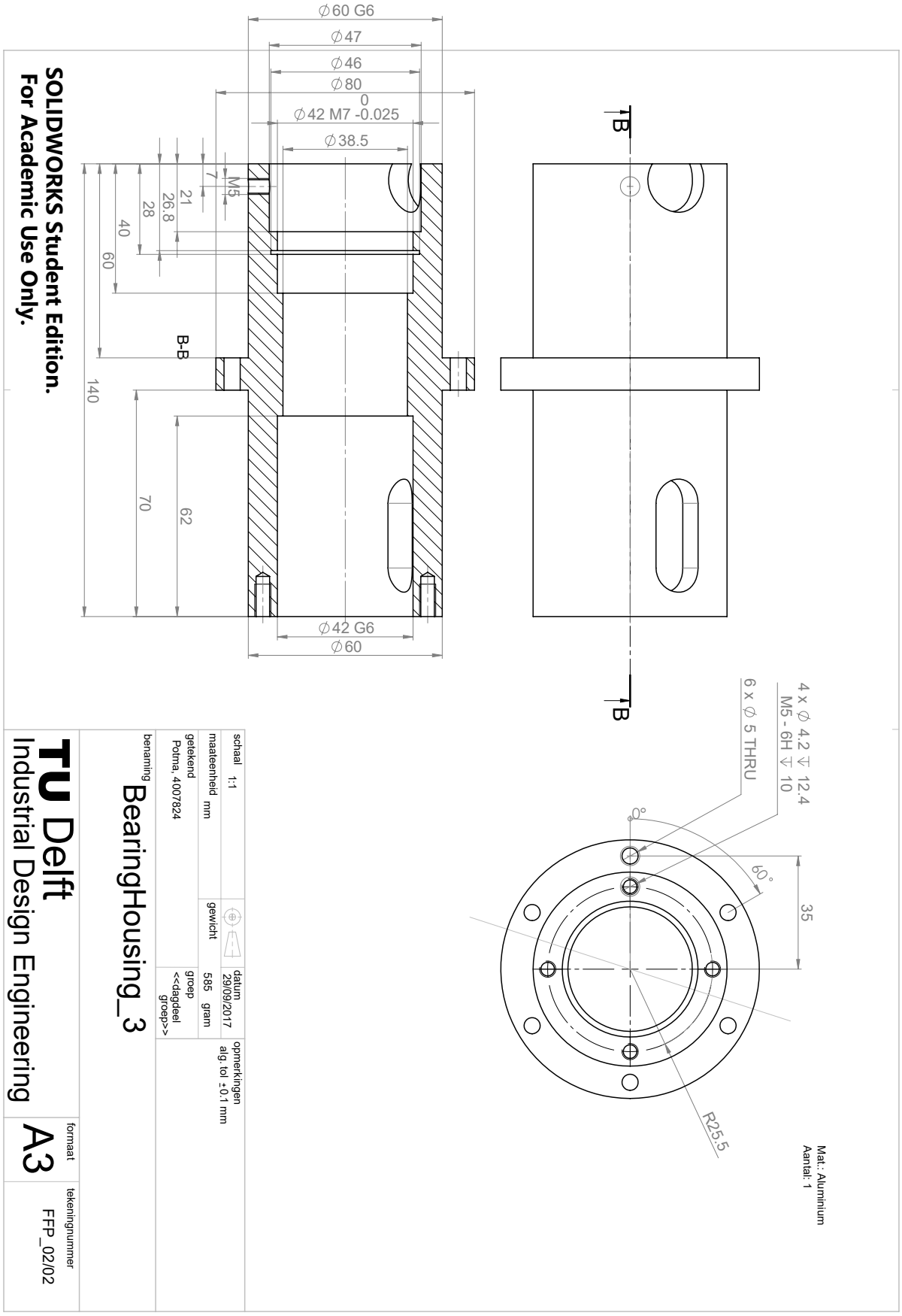

Figure D.3: Blueprint of the shaft housing

Figure D.4: Blueprint of the shaft

Figure D.5: Blueprint of the magnet holder

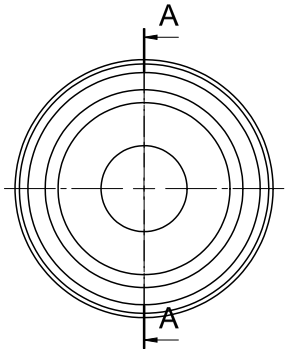

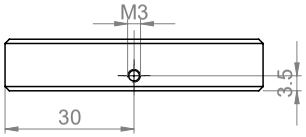

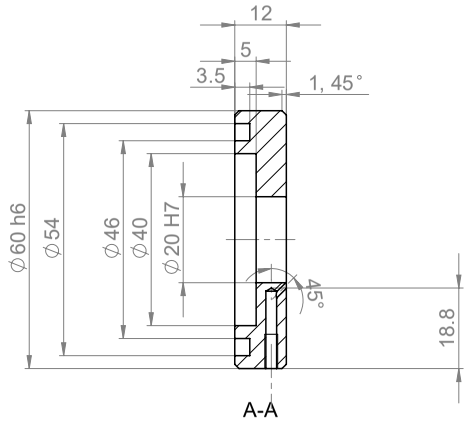

Mat.: Aluminium
Aantal: 1

schaal 1:1		datum 29/09/2017	opmerkingen randen breken, alg. tol. +- 0.1mm
maateenheid mm	gewicht 62 gram		
getekend Potma, 4007824		groep <<dagdeel groep>>	
benaming Shield_3			
TU Delft Industrial Design Engineering		formaat A3	tekeningnummer FFP_02/05

Figure D.6: Blueprint of the shield

Figure D.7: Blueprint of the reservoir cover

Figure D.8: Blueprint of the flange that couples the motor with the setup.

Appendix E

Power calculation

To have an idea on what is needed to effectively drive the experiments of the setup a basic calculation can be made on the power consumption of the setup. the folling appendix is on all the steps required to make an educated guess on the strength of the motor to be used in the experiments.

E.1 Shear stress

The Shear stress is acting on the surface area of the shaft where the fluid makes contact. The areas of interest are the the seals and the shield. Other contact parts are negligible.

$$A_{seal} = \pi d_s b_{seal} N \tag{E.1}$$

$$A_{shield} = \pi d_s b_{shield} \tag{E.2}$$

Here d_s is the diameter of the shaft, b is the width of the contact area of the seal or shield and N are the amount of seals. The shear stress is dependent on the dynamic viscosity of the fluid μ, the peripheral speed v, and the gapsize between the moving and stationary parth_G. the last term shows that only small gapsizes are of interest for large gapsizes become negligibly small. The calculation of bothe the shear stress in a seal and shield are give respectively.

$$\tau_{FF} = \frac{\mu_{FF} \cdot v}{h_G} \tag{E.3}$$

$$\tau_{water} = \frac{\mu_{water} v}{h_G} \tag{E.4}$$

E.2 Torque

The required torque comes from several sources. The seal assembly itself is dependent of the shear stress times the surface area.

$$T_{seals} = \tau_{FF} A_{seal} \tag{E.5}$$

$$T_{shield} = \tau_{water} A_{shield} \tag{E.6}$$

The bearing torque is calculated using the manual from SKF. Here $\mu_{bearing}$ is the friction coefficient, F_{dyn} is the predicted dynamic bearing load, and d_{bore} is the bore diameter of the bearing, i.e. the inner ring diameter.

$$T_{bearing} = 0.5 \mu_{bearing} * 0.1 * F_{dyn} * d_{bore} \tag{E.7}$$

To protect the bearing from the FF, the chosen type has lipseal covers that add to the required torque. The parameters are all dependent on the bearing type and size and can be looked up in the manual of SKF

$$T_{lipseal} = k_{s1} d_2^{\beta} + k_{s2} \tag{E.8}$$

The total required torque is a summation of the seal assembly, the two bearings and the lipseal. A remark on the equation is that the equations of SKF are calculated in Nmm and thus have a conversion to bring it to Nm.

$$T_{Tot} = T_{seals} + T_{shield} + (2T_{bearing} + T_{lipseal}) * 1e^{-3} \tag{E.9}$$

E.3 Power

Power consumption of the setup is again devided in the seal assembly and the bearings. for the seal assembly the power is dependent on the peripheral speed, the torque and the shaft diameter. The power consumption of the bearings and seal are once again taken from the SKF manual.

$$P_{seals} = \frac{vT_{seals}}{\frac{d_s}{2}} \tag{E.10}$$

$$P_{shield} = \frac{vT_{Shield}}{\frac{d_s}{2}} \tag{E.11}$$

$$P_{bearing} = \frac{60vT_{bearing}}{\pi d_s} 1.05e^{-4} \tag{E.12}$$

$$P_{lipseal} = \frac{60vT_{lipseal}}{\pi d_s} 1.05e^{-4} \tag{E.13}$$

With this the total power consumption can be calculated and gives insight into the type of electic motor that is needed to power the setup.

$$P_{tot} = P_{seals} + P_{shield} + 2P_{bearing} + P_{lipseal} \tag{E.14}$$

E.4 Calculation

In calculating the power consumption that the motor needs to be able to handle,the values for the parameters have been chosen as seen in table E.4. For the speed a array of increasing speeds have been chosen to visualise the consumption per speed.The result is a power array

$$P_{tot} = [8.6527 \quad 20.4470 \quad 35.382853.4603 \quad 74.6794 \quad 99.0400] \quad W$$

Table E.1: Parameters used in calculating the power consumption

parameter	value
v	[1 2 3 4 5 6] m/s
μ_{FF}	0.006 Pa.s
μ_{water}	0.001 Pa.s
N	3
b_{seal}	0.001 m
b_{shield}	0.007 m
d_s	0.01985 m
$\mu_{bearing}$	0.0015
h_G	0.0001 m
$\mu_{bearing}$	0.0015
F_{dyn}	9950 N
d_{bore}	20 mm
k_{s1}	0.028
d_2	24.9 mm
β	2.25
k_{s2}	2

Appendix F

SEW motor installation

This appendix is a short overview of the neccersary knowledge for controlling the SEW motor. It contains a list of all components for assembly, as well as the cables, drivers and other software. experiences obtained with working with the motor control will be added to where applicable.

F.1 Parts

The following table contains all parts used in the installation.

Table F.1: Motor installation components

component	comment
SEW Synchroonmotor	CMP40S/KY/RH1M/SM1/6000RPM
encoder	MDX61B0005-5A3-4-00/DER11B
power cable	3m prefabricated
controller cable	3m prefabricated
interface adapter set	USB11A
Installation DVD (3x)	
control panel	DBG60B-01

F.2 Installation

Call the SEW service line and have them help you correctly configure the motor. Use the Movidrive MDX60-61B Operating Instructions and Movidrive MDX60-61B system manual manuals found on internet as guides. Install the Movidrive studio software from the provided DVD.

F.3 Control

The motor can be controlled manually in the Movidrive software by selecting the motor and opening the manual mode. In here the motor can be activated. the speed can now be controlled. Important to always deactivating the motor before closing the program, for this can result in error in the inverter.

Appendix G

Magnetism

In a seal the shaft rotates in a magnetic field. The movement of conducting material through a field creates eddy currents which induces an opposing force, leading to losses and thus to resistance. A way to find the amount of energy loss is a rotating system is to find out what the joule heating is. To start, the flux density of a magnetic field is expressed as

$$B = \mu_0(H + M) \tag{G.1}$$

This can be simplified due to linear approximations

$$B \approx \mu_0\mu_r H \approx \mu H \tag{G.2}$$

The flux is then obtained with the following expression

$$\phi_m = \int_S B \cdot n \, dA \tag{G.3}$$

With Faraday's law the electromotive force (emf) is obtained caused by the magnetic flux

$$\varepsilon = -\frac{d\phi_m}{dt} = -\frac{d}{dt}\int_S B \cdot n \, dA \tag{G.4}$$

The emf is then used to calculate the joule heating

$$P = I^2R = \frac{\varepsilon^2}{R} \tag{G.5}$$

When analysing the movement of the shaft in the magnetic field it becomes obvious that the movement does not change the flux going through the material over time, making the emf equal to zero. This shows that no energy is lost specifically by joule heating.

Appendix H

Magnetization test

In checking the datasheet provided with the FF the magnetization curve is measured in a increasing magnetic field.as a result the magnetic saturation of the FF can be determined. The field is increased in the sample incrementally and the magnetic moment is measured. To convert the field to [kA/m]

$$1 \quad Oe = 1/4\pi \quad kA/m \tag{H.1}$$

or to [mT] with

$$1 \quad Oe = 0.1 \quad kA/m \tag{H.2}$$

The magnetic moment τ can be converted to magnetization strength by first finding the volume of the sample

$$V = m/\rho \tag{H.3}$$

where $m = 11150mg$ is the mass o the sample and $\rho = 1210mg/cm^3$ is the density. Next the moment is divided by the volume to get the magnetization strength

$$M = \tau/V \tag{H.4}$$

and converted to [mT] with

$$1 \quad kA/m = 4\pi.10^{-1} \quad mT \tag{H.5}$$

In table H.1 the results from the test have been displayed and in figure H.1 the magnetization curve is displayed. From this a magnetic saturation of the FF is found of $M_s = 0.042mT$, wich corresponds with the ... of the data sheet.

Table H.1: The applied field in [Oe] is converted to [kA/m] and mT. The measured magnetic torque is converted to [kA/m] and [mT]

Field [Oe]	Field [kA/m]	field [mT]	Mag. Torque [emu]	Magnetization strength [kA/m]	Magnetization strength [mT]
0	0	0	0.0010	0.00010	0.00013
100	7.957	10	0.0781	0.00848	0.01066
200	15.915	20	0.1313	0.01425	0.01790
300	23.873	30	0.1627	0.01766	0.02219
400	31.831	40	0.1824	0.01980	0.02488
500	39.789	50	0.1968	0.02136	0.02684
600	47.746	60	0.2079	0.02256	0.02835
700	55.704	70	0.2168	0.02352	0.02956
800	63.662	80	0.2240	0.02431	0.03055
900	71.612	90	0.2301	0.02497	0.03137
1000	79.577	100	0.2352	0.02552	0.03207
2000	159.155	200	0.2635	0.02860	0.03594
3000	238.732	300	0.2759	0.02994	0.03763
4000	318.310	400	0.2832	0.03073	0.03862
5000	397.887	500	0.2881	0.03126	0.03928
6000	477.465	600	0.2916	0.03165	0.03977
7000	557.042	700	0.2944	0.03194	0.04014
8000	636.620	800	0.2965	0.03218	0.04044
9000	716.197	900	0.2983	0.03237	0.04068
10000	795.775	1000	0.2998	0.03254	0.04089
17500	1392.606	1750	0.3065	0.03326	0.04180
20000	1591.549	2000	0.3078	0.03340	0.04198

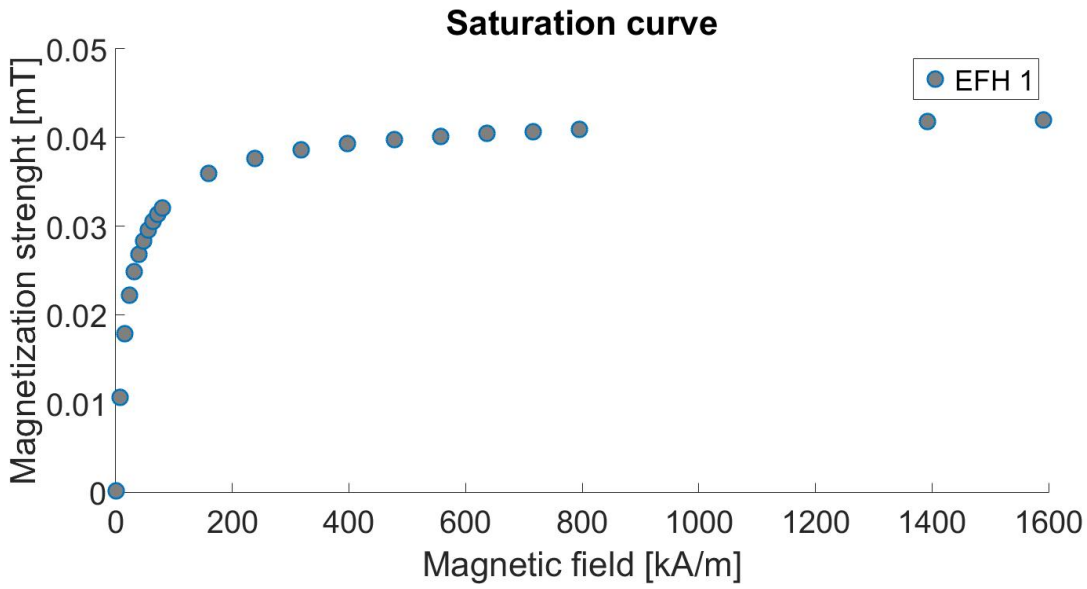

Figure H.1: The curve shows the saturation of the FF with increasing magnetic field.

Bibliography

[1] J Kurfess and H.K. Müller. Sealing liquids with magnetic liquids. *Journal of Magnetism and Magnetic Materials*, 85:246–252, 1990.

[2] K. Raj, P. Stahl, and W. Bottenberg. Magnetic Fluid Seals for Special Applications. *A S L E Transactions*, 23(4):422–430, 1980.

[3] I. Anton, I. De Sabata, L. Vékás, I. Potencz, and E. Suciu. Magnetic fluid seals: Some design problems and applications. *Journal of Magnetism and Magnetic Materials*, 65(2-3):379–381, 1987.

[4] Zou Jibin and Lu Yongping. Numerical Calculations for Ferrofluid Seals. *IEEE Transactions on Magnetics*, 28(6):3367–3371, 1992.

[5] Jim Bonvouloir. Experimental Study of High Speed Sealing Capability of Single Stage Ferrofluidic Seals. *Journal of Tribology*, 119(96):416–421, 1997.

[6] Wlodzimierz Ochonski. New designs of magnetic fluid exclusion seals for rolling bearings. *Industrial Lubrication and Tribology*, 57(3):107–115, 2005.

[7] V. Polevikov and L. Tobiska. Influence of diffusion of magnetic particles on stability of a static magnetic fluid seal under the action of external pressure drop. *Communications in Nonlinear Science and Numerical Simulation*, 16(10):4021–4027, 2011.

[8] W Horak and M Szczęch. Experimental and numerical determination of the static critical pressure in ferrofluid seals. *Journal of Physics: Conference Series*, 412:012055, 2013.

[9] R A Williams and E. Malsky. Some experiences using a ferrofluid seal against liquid. *IEEE Transactions on Magnetics*, Mag-16(2):379–381, 1980.

[10] Yoshinori Mitamura, Sayaka Takahashi, Shuichi Amari, Eiji Okamoto, Shun Murabayashi, and Ikuya Nishimura. A magnetic fluid seal for rotary blood pumps: Effects of seal structure on long-term performance in liquid. *Journal of Artificial Organs*, 14(1):23–30, 2011.

[11] Yoshinori Mitamura, Tetsuya Yano, Wataru Nakamura, and Eiji Okamoto. A magnetic fluid seal for rotary blood pumps: Behaviors of magnetic fluids in a magnetic fluid seal. *Bio-Medical Materials and Engineering*, 23(1-2):63–74, 2013.

[12] Tonggang Liu, Yusheng Cheng, and Zhiyi Yang. Design optimization of seal structure for sealing liquid by magnetic fluids. *Journal of Magnetism and Magnetic Materials*, 289:411–414, 2005.

[13] Zbigniew Szydło and Leszek Matuszewski. Experimental Research on Effectiveness of the Magnetic Fluid Seals for Rotary Shafts Working in Water. *Polish Maritime Research*, 14(4):53–58, 2007.

[14] Leszek Matuszewski. Multi-stage magnetic-fluid seals for operating in water âĂŞ life test procedure, test stand and research results Part I. *Polish Maritime Research*, 19(May):62–70, 2012.

[15] T. Borbáth, D. Bica, I. Potencz, L. Vékás, I. Borbáth, and T. Boros. Magnetic nanofluids and magnetic composite fluids in rotating seal systems. *IOP Conference Series: Earth and Environmental Science*, 12(5):012105, 2010.

[16] Marcin Szczech and Wojciech Horak. Tightness testing of rotary ferromagnetic fluid seal working in water environment. *Industrial Lubrication and Tribology*, 67(5):455–459, 2015.

[17] Stefan Georges Emile Lampaert. Planar Ferrofluid Bearings Modelling and Design Principles. (December), 2015.

[18] Paul A. Tipler. *Physics for Scientist and Engineers*. 2008.

[19] Stefan Odenbach. Recent progress in magnetic fluid research. *Journal of Physics: Condensed Matter*, 16(32):R1135–R1150, 2004.

[20] Stefan Odenbach. Magnetoviscous and Viscoelastic Effects in Ferrofluids. *International Journal of Modern Physics B*, 14(16):1615–1631, 2000.

[21] R E Rosensweig. Magnetic Fluids. *Annual Review of Fluid Mechanics*, 19(1):437–461, 1987.

[22] P. Dullemond. 9 Fluid Instabilities. 0:1–5.

[23] Ronald E. Rosensweig. *Ferrohydrodynamic Instabilities*. Number October. 1985.

[24] Wlodzimierz Ochonski. Dynamic sealing with magnetic fluids. *Wear*, 130(1):261–268, 1989.

[25] K. Raj, B. Moskowitz, and R. Casciari. Advances in ferrofluid technology. *Journal of Magnetism and Magnetic Materials*, 149(1-2):174–180, 1995.

[26] D. Li, H. Zhang, and Z. Zhang. Study on Magnetic Fluid Static Seal of Large Gap. *Key Engineering Materials*, 512-515:1448–1454, 2012.

[27] Hiroshi Tamama, Yukio Ozawa, Hiroshi Ito, and Toyohiro Kinoshita. DEVICE FOR SEALING A PROPELLER SHAFT AGAINST INVASION OF SEA FOREIGN PATENT DOCUMENTS WATER, 1984.

[28] Yoshinori Mitamura, K Sekine, M Asakawa, R Yozu, S Kawada, and E Okamoto. A durable, non power consumptive, simple seal for rotary blood pumps. *ASAIO Journal*, 47(4):392–396, 2001.

[29] Yoshinori Mitamura, Sayaka Takahashi, Kentaro Kano, Eiji Okamoto, Shun Murabayashi, Ikuya Nishimura, and Taka Aki Higuchi. Sealing Performance of a Magnetic Fluid Seal for Rotary Blood Pumps. *Artificial Organs*, 33(9):770–773, 2009.

[30] Yoshinori Mitamura, Sayaka Takahashi, Shuichi Amari, Eiji Okamoto, Shun Murabayashi, and Ikuya Nishimura. A magnetic fluid seal for rotary blood pumps: Long-term performance in liquid. *Physics Procedia*, 9(2):229–233, 2010.

[31] Leszek Matuszewski and Zbigniew Szydło. The application of magnetic fluids in sealing nodes designed for operation in difficult conditions and in machines used in sea environment. 15(3):49–58, 2008.

[32] Leszek Matuszewski and Zbigniew Szydlo. Life tests of a rotary single-stage magnetic-fluid seal for shipbuilding applications. *Polish Maritime Research*, 18(2):51–59, 2011.

[33] Leszek Matuszewski. Multi-stage magnetic-fluid seals for operating in water âĂŞ life test procedure, test stand and research results Part II. *Polish Maritime Research*, 20(May):39–47, 2013.